HEINRICH HEINE
UNIVERSITÄT
DÜSSELDORF

Unraveling the mechanisms of EGFR-inhibitor associated cutaneous adverse effects

Inaugural-Dissertation

zur Erlangung des Doktorgrades
der Mathematisch-Naturwissenschaftlichen Fakultät
der Heinrich-Heine-Universität Düsseldorf

vorgelegt von

Bettina Alexandra Buhren

aus Dinslaken

Düsseldorf, Dezember 2009

Aus der Hautklinik,
Forschungslabor für Dermato-Immunologie und Onkologie
der Heinrich-Heine-Universität Düsseldorf

Gedruckt mit der Genehmigung der
Mathematisch-Naturwissenschaftlichen Fakultät der
Heinrich-Heine-Universität Düsseldorf

Referent: Univ.-Prof. Dr. Bernhard Homey
Koreferent: Univ.-Prof. Dr. Dieter Willbold

Tag der mündlichen Prüfung: 29.01.2010

Table of Contents

1 Summary

Recently, antagonists directed against the epidermal growth factor receptor (EGFR) have been successfully established in the treatment of cancer. Papulo-pustular rashes often accompanied by bacterial superinfections are considered the most prominent and most frequent adverse effects related to these targeted cancer drugs. Despite their clinical relevance the underlying molecular and cellular mechanisms of these adverse events have remained largely elusive.

In the present study, the molecular and cellular mechanisms underlying EGFR-inhibitor (EGFR-I) associated cutaneous adverse events were analyzed. First, the inflammatory infiltrate and microbial colonization of EGFR-I induced rashes were systematically characterized and subsequently, the expression of chemokines and antimicrobial peptides in the presence or absence of EGFR-I was assessed *in vitro* and *in vivo*.

The inflammatory infiltrate of early stages of EGFR-I-induced skin eruptions is dominated by $CD1a^+$ Langerhans cells, $CD68^+$ macrophages, and $CD4^+$ T lymphocytes. In addition, the skin eruptions frequently showed a marked colonization with *Staphylococcus aureus* (*S. aureus*). Correspondingly, EGFR-I selectively induced the expression of proinflammatory and skin-associated chemokines (CCL5, CCL27, and CXCL14) in human primary keratinocytes while the production of antimicrobial peptides (LL37, HBD3, RNAse7) was significantly suppressed. Functional analyses confirmed that conditioned media of EGFR-I treated keratinocytes expose a strong chemotactic potential on relevant leukocyte subsets. Moreover, the retinoid isotretinoin was able to suppress the EGFR-I induced chemokine production in *vitro*. The findings suggest a dual role for the EGFR at the interface between the host and the environment controlling inflammation and sustaining host defense within epithelial surfaces. Based upon the results of this thesis a novel model for the mechanisms of action of EGFR-I induced cutaneous adverse effects is proposed combining the induction of proinflammatory chemokines on the one and the suppression of antimicrobial peptides on the other hand.

2 Introduction

2.1 Epidermal Growth Factor Receptor (EGFR)

The epidermal growth factor receptor (EGFR) signaling pathway is a key regulator of growth, survival, proliferation, and differentiation in mammalian cells. The EGFR family of receptor tyrosine kinases (RTKs) includes four members: EGFR (HER1 or ErbB1) (Ullrich *et al.* 1984), ErbB2 (Neu or HER2) (Coussens *et al.* 1985, Schechter *et al.* 1984), ErbB3 (HER3) (Kraus *et al.* 1989, Plowman *et al.* 1990), and ErbB4 (HER4) (Plowman *et al.* 1993). The EGFR is a 170 kDa transmembrane protein that consists of a glycosylated and disulfide-bonded extracellular domain, a single hydrophobic transmembrane domain, and an intracellular domain with a tyrosine kinase and multiple phosphorylation sites. The extracellular region can be divided into four domains: I-IV. Domains I and III participate in ligand binding whereas the cysteine rich domains II and IV participate in receptor dimerization (Hynes & Lane 2005).

2.1.1 Ligands

Activation of the EGFR is regulated by a selective and specific interaction with members of the EGF-like peptide growth factor family: epidermal growth factor (EGF) (GrayDull & Ullrich 1983, Savage & Cohen 1972), heparin binding EGF-like growth factor (HB-EGF) (Higashiyama *et al.* 1991), transforming growth factor-α (TGF-α) (Derynck *et al.* 1984), betacellulin (BTC) (Sasada *et al.* 1993), amphiregulin (AR) (Shoyab *et al.* 1989), epiregulin (EPR) (Toyoda *et al.* 1995), and epigen (EPG) (Strachan *et al.* 2001). Each ligand contains an EGF-like domain that determines its binding specificity. ErbB ligands are synthesized as transmembrane precursors processed by proteolytic cleavage at the cell surface to release a mature soluble ectodomain referred to as “ectodomain shedding”. Members of the ADAM (a disintegrin and metalloproteinase) family and matrix metalloproteinases (MMPs) are involved in ectodomain shedding of ErbB ligands (SandersonDempsey & Dunbar 2006).

2.1.2 Signaling

Ligand binding to the extracellular domain of the EGFR leads to conformational changes and receptor dimerization. Ligand-induced dimerization results in activation of the intrinsic kinase domain and auto-phosphorylation of tyrosine residues in the intracellular domain. Subsequently, recruitment of signaling molecules to the phosphorylated tyrosine residues induces the activation of downstream signaling cascades (Mendelsohn & Baselga 2006, Yarden & Sliwkowski 2001). These signaling pathways include (*a*) the Ras-Raf mitogen-activated protein kinase (MAPK) mitogenic pathway, (*b*) the phosphatidylinositol 3-kinase-AKT cell survival pathway, and (*c*) stress-activated protein kinase C and Jak/Stat pathway (Mendelsohn & Baselga 2006, Yarden & Sliwkowski 2001).

2.2 Expression and function of the EGFR in the skin

The EGFR is widely expressed on cells of both epithelial and mesenchymal lineages (Wells 1999). Besides regulating normal cell growth and differentiation when dysregulated the EGFR and its ligands are involved in the molecular pathogenesis of cancer either via elevated expression levels or through mutation (Jorissen *et al.* 2003, Yarden & Sliwkowski 2001).

Normal skin is composed of three layers: the epidermis (the most superficial layer), the dermis (providing support and tensile strength), and the subcutis (adipose tissue).

In the epidermis, keratinocytes account for approximately 90% of all structural cells. These cells proliferate in the *Stratum basale* and undergo strictly regulated processes of differentiation and migration as they pass the *Stratum spinosum*, the *Stratum granulosum*, and the *Stratum corneum* which is the most external layer. The EGFR is primarily expressed by undifferentiated, proliferating keratinocytes in the basal and suprabasal layers of the epidermis as well as in the outer root sheath of hair follicles (Green *et al.* 1983, Green & Couchman 1984, Hansen *et al.* 1997).

When keratinocytes exit the basal layer, the expression of EGFR is lost which is a process that is characterized by growth arrest and initiation of differentiation.

Observation in mouse models exposing either decreased EGFR activity or non-functional EGFR highlight the importance of EGFR signaling in epidermal development. Those mice display various epidermal defects like skin atrophy, premature skin, or hair abnormalities (Miettinen *et al.* 1995, Sibilia & Wagner 1995, Threadgill *et al.* 1995).

2.3 EGFR and its role in cancer (pharmacotherapy)

The EGFR was the first RTK directly associated with human cancer (GschwindFischer & Ullrich 2004). In 1984, analyses of the EGFR peptide and sequence revealed a high level of similarity to an avian oncogene, v-erbB (Downward *et al.* 1984). In particular, the activation of the EGFR has been associated with tumorigenesis. Amplification or increased transcription of the EGFR gene, leading to an overexpression, have been detected in a variety of different solid human cancers such as colorectal cancer, pancreatic cancer, squamous cell carcinoma of the head and neck (HNSCC), and non-small cell lung cancer (NSCLC) (Salomon *et al.* 1995). Accumulating evidence suggests a direct correlation between the level of EGFR overexpression and the active proliferation of malignant cells as well as a poor prognosis of patients (Bianchi *et al.* 2006, Dassonville *et al.* 1993).

A significant fraction of EGFR expressing tumors show in-frame deletions and point mutations that result in increased catalytic tyrosine-kinase activity of the receptor (Humphrey *et al.* 1990). The most common mutation EGFRvIII that arises from gene rearrangement or alternative mRNA splicing, which is frequently found in glioblastomas, results in a protein with a defective ligand binding capacity, leading to constitutive kinase activity and enhanced tumorigenicity (Nishikawa *et al.* 1994, Pedersen *et al.* 2001). Treatment strategies that inhibit the RTK domain or block binding of ligands to the receptor's extracellular domain have recently emerged as promising therapies in cancer.

2.4 EGFR targeted cancer drugs

EGFR research has led to the development of targeted cancer drugs including anti-EGFR monoclonal antibodies (mAbs) directed against the receptor extracellular domain as well as low molecular weight tyrosine-kinase inhibitors (TKIs) that are directed against the intracellular tyrosine kinase domain) (Figure 2.1).

Cancer drugs that target the EGFR, such as erlotinib (Tarceva®, Roche), gefitinib (Iressa®, AstraZeneca) or cetuximab (Erbitux®, Merck) have been approved for clinical use in the treatment of various tumor entities.

2.4.1 Small molecule tyrosine kinase inhibitors

Erlotinib (previously known as OSI-774 and CP-358774) is an orally active (150 mg orally once daily) small molecule weight inhibitor which blocks the EGFR tyrosine kinase activity (Moyer *et al.* 1997, Pollack *et al.* 1999). Erlotinib shows promising anti-cancer effects in a variety of preclinical cancer models. It affects the growth of tumor cells such as squamous cell carcinoma cells of the head and neck in *in vitro* and *in vivo* studies. In Germany and in the United States of America, erlotinib has been approved for the treatment of locally advanced and metastatic non-small-cell lung cancer (NSCLC) and metastatic pancreatic cancer (www.fda.gov).

Erlotinib competes with the binding of ATP to the intracellular tyrosine kinase domain of the EGFR. Thereby it inhibits receptor autophosphorylation and blocks downstream signal transduction (Moyer et al. 1997).

2.4.2 Antibodies

The chimeric human/murine monoclonal antibody cetuximab binds to the extracellular domain of the EGFR. It competes with physiological EGFR ligands for receptor occupation thereby blocking tyrosine kinase phosphorylation and promoting receptor internalization (Gill *et al.* 1984, Goldstein *et al.* 1995, Sato *et al.* 1983, Sunada *et al.* 1986). It has been shown to inhibit tumor growth of various tumor xenografts including prostate, colon, and renal carcinoma (Ciardiello *et al.* 2001). In Germany and in the Unites States of America,

cetuximab has received approval as a second-line therapy for the treatment of metastasized colon carcinoma in 2004 as well as for the treatment of advanced squamous cell carcinoma (HNSCC) of the head and neck.

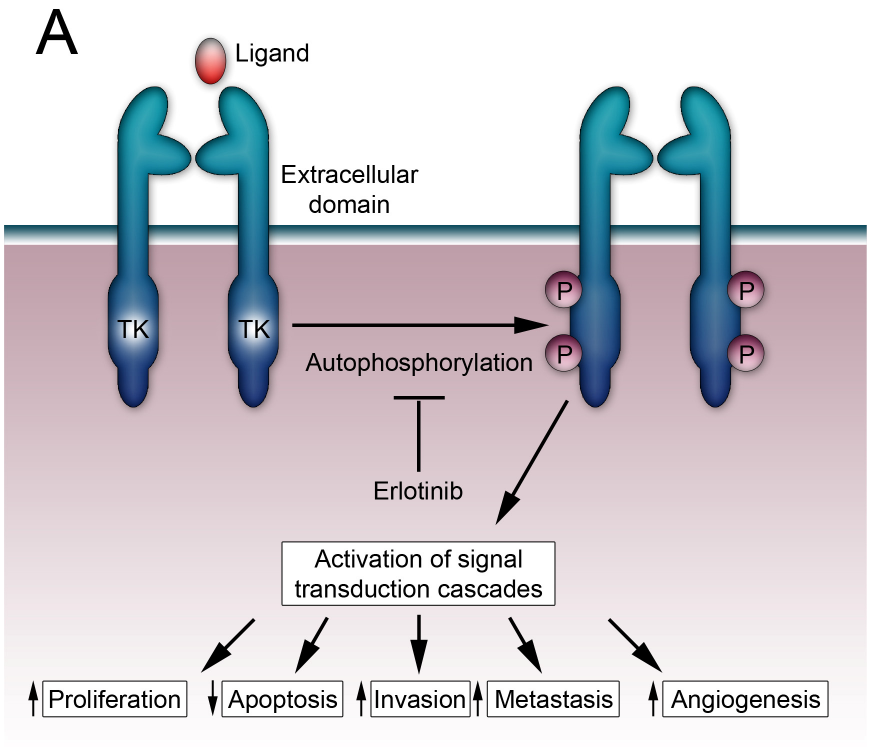

B

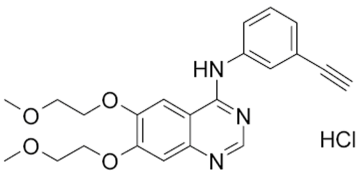

Erlotinib hydrochloride

IUPAC name: N-(3-Ethinylphenyl)-6,7-bis-(2-methoxyethoxy)chinazolin-4-amin

Fomula: $C_{22}H_{23}N_3O_4 \cdot HCl$

Molecular weight: 429.907g/mol

Figure 2.1 Mechanism of action of erlotinib. Erlotinib is a reversible inhibitor of the receptor tyrosine kinase domain of EGFR that competes with ATP for binding to the catalytic pocket. It inhibits EGFR autophosphorylation, thus inhibiting receptor dimerization and the downstream signaling that would have otherwise stimulated proliferation and anti-apoptotic mechanisms. Adapted and modified from (DowellMinna & Kirkpatrick 2005)

2.5 EGFR-I induced cutaneous adverse effects

EGFR targeting therapies are typically well tolerated and are rarely associated with severe systemic adverse effects. However, frequent side effects of EGFR-I include skin toxicities like extensive papulo-pustular eruptions that are characterized by follicular-based erythematous papules and pustules (rash). Besides these well-known so called 'acneiform eruptions', xerosis (leading to eczema and fissures), paronychia, hair changes, telangiectasia, hyperpigmentation, and mucosal changes may occur (Arteaga 2001, Ciardiello & Tortora 2002, Jacot *et al.* 2004, Salomon et al. 1995). The distribution is primarily limited to the face, neck, and upper trunk (Figure 2.2). Skin toxicities affect approximately two thirds of patients treated with EGFR-I usually beginning during the first 2 weeks of therapy. Often they are dose dependent (Soulieres *et al.* 2004) and resolve with discontinuation of EGFR-I therapy (Perez-Soler *et al.* 2004). However, they can spontaneously resolve despite continued treatment (Hidalgo *et al.* 2001). Although little is known about their etiology and pathogenesis, there is accumulating evidence that the degree of rash outcome is positively correlated with improved clinical response and/or prolonged survival (Herbst *et al.* 2005).

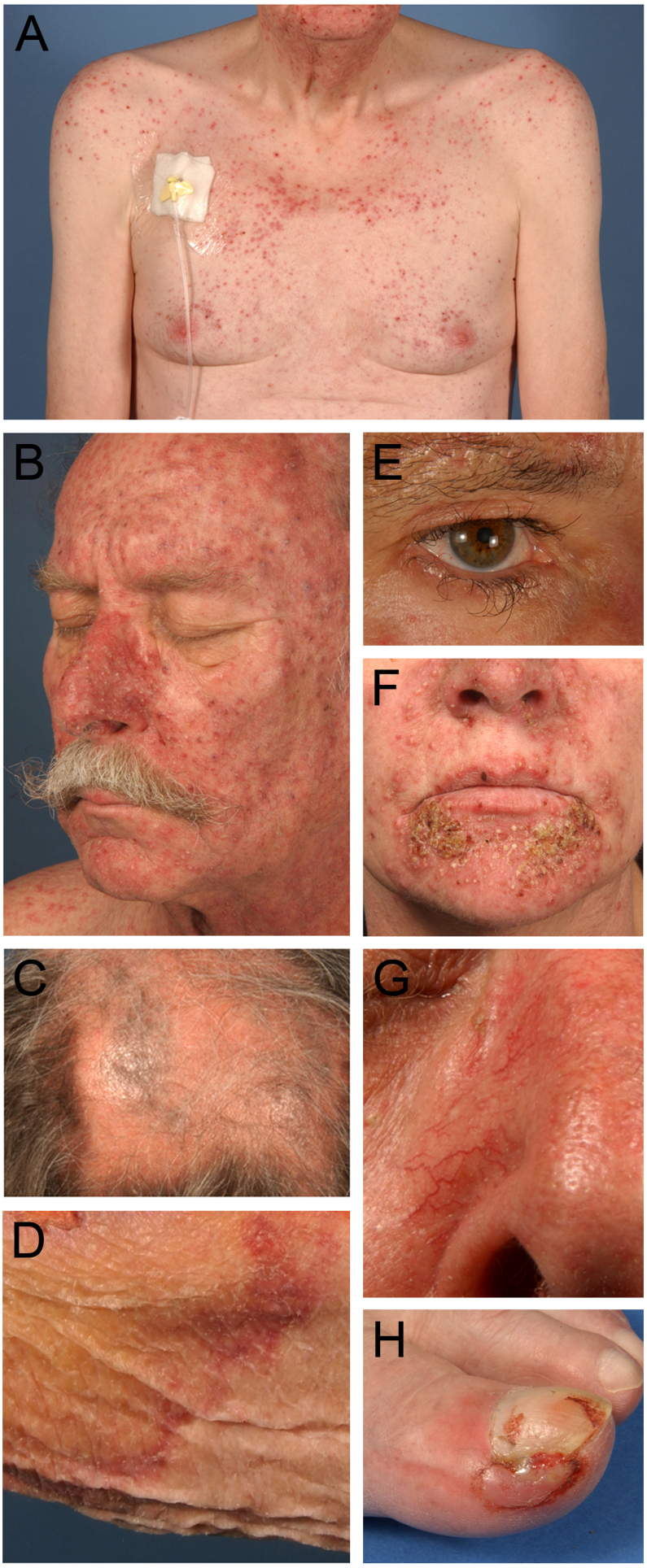

Figure 2.2 EGFR-I induced cutaneous side-effects: (A, B) Papulo-pustular exanthema („acneiform rash“) located to the trunk and head. (C) Non-scarring diffuse alopecia. (D) Skin atrophy. (E) Alterations of the hair structure. (F) Perioral papulo-pustular exanthema with confluating pustules and yellowish crusts. (G) Telangiectasia. (H) Paronychia.

2.6 Skin inflammation

The skin epithelium represents a major barrier between the host and the external environment. Consequently, it is adequately equipped to induce an effective immune response against microorganisms and other environmental threads like physical, chemical, or immune-specific insults.
It is mainly composed of keratinocytes, mast cells, and endothelial cells constituting the static components of the skin immune system which are interspersed with dendritic cells (DCs) including epidermal Langerhans cells (LCs) and dermal DCs, rare T lymphocytes, and monocytes.
The induction of an immune response is initiated with an increased expression of a system of proinflammatory mediators including a variety of chemoattractants which leads to the recruitment of distinct leukocyte subpopulations to the site of skin inflammation. In turn, activated monocytes, DCs, and T cells release potent cytokines that act on cells in the local environment to boost the inflammatory response (Pastore *et al.* 2005).
Dermatohistopathological analyses of the inflammatory skin eruptions in EGFR-I treated patients display an extensive folliculitis and perifolliculitis. The dense inflammatory infiltrate consists of T lymphocytes, neutrophilic lymphocytes, eosinophilic granulocytes and macrophages. The trafficking of these effector cells is mainly mediated by the protein family of chemokines (Charo & Ransohoff 2006, Zlotnik & Yoshie 2000). Various studies have proven the important role of chemokines in the pathogenesis of inflammatory skin diseases like atopic eczema or psoriasis vulgaris (Homey & Bunemann 2004, Homey & Meller 2008, Homey *et al.* 2006, LowesBowcock & Krueger 2007).
In particular, the proinflammatory cytokine tumor necrosis factor-alpha (TNF-α) induces the expression of numerous chemokines including CCL27, CCL5, CCL2, CCL20, CXCL8, and CXCL10 in keratinocytes.

2.7 Chemokines

Chemokines represent a superfamily of structurally related small (6-14 kDa), cytokine-like proteins that regulate the trafficking of leukocytes including lymphocytes, DCs, monocytes, neutrophils, and eosinophils. Chemokines are

classified into four subclasses according to the position of two highly conserved cysteine residues at the N-terminus of the molecule: the C-C, C-X-C, C and C-X3-C chemokines. Besides their main function, the regulation of cell trafficking, chemokines also play important roles in inducing leukocyte activation and differentiation (HomeyMuller & Zlotnik 2002, Rossi & Zlotnik 2000, Zlotnik & Yoshie 2000). The biological effects of chemokines on target cells are mediated by the interaction with their receptors which belong to a superfamily of seven transmembrane G protein-coupled receptors (GPCRs), (Murphy *et al.* 2000).

To date, 45 human chemokines and 19 receptor encoding genes have been identified (Figure 2.3).

Binding of chemokines to their specific receptor is often highly promiscuous as a single chemokine can bind different receptors and a chemokine receptor can be activated by distinct chemokines. In contrast, some chemokines show a very high receptor as well as tissue specificity. Particularly, CCL27 is predominantly expressed in the skin by epidermal basal keratinocytes and binds specifically to the CCR10 receptor (Homey *et al.* 2002).

Depending on the function and site of production chemokines can be classified as inflammatory or homeostatic. Inflammatory chemokines can be induced by pathogens and proinflammatory stimuli. They are expressed in inflamed tissues by both resident tissue cells and infiltrating leukocytes thereby recruiting effector cells. On the other hand, homeostatic chemokines are constitutively expressed in lymphoid tissues, skin, and mucosa. They are involved in the maintenance of basal leukocyte trafficking and homing as well as in developmental processes (Baggiolini 2001, HomeyMuller & Zlotnik 2002, Zlotnik & Yoshie 2000).

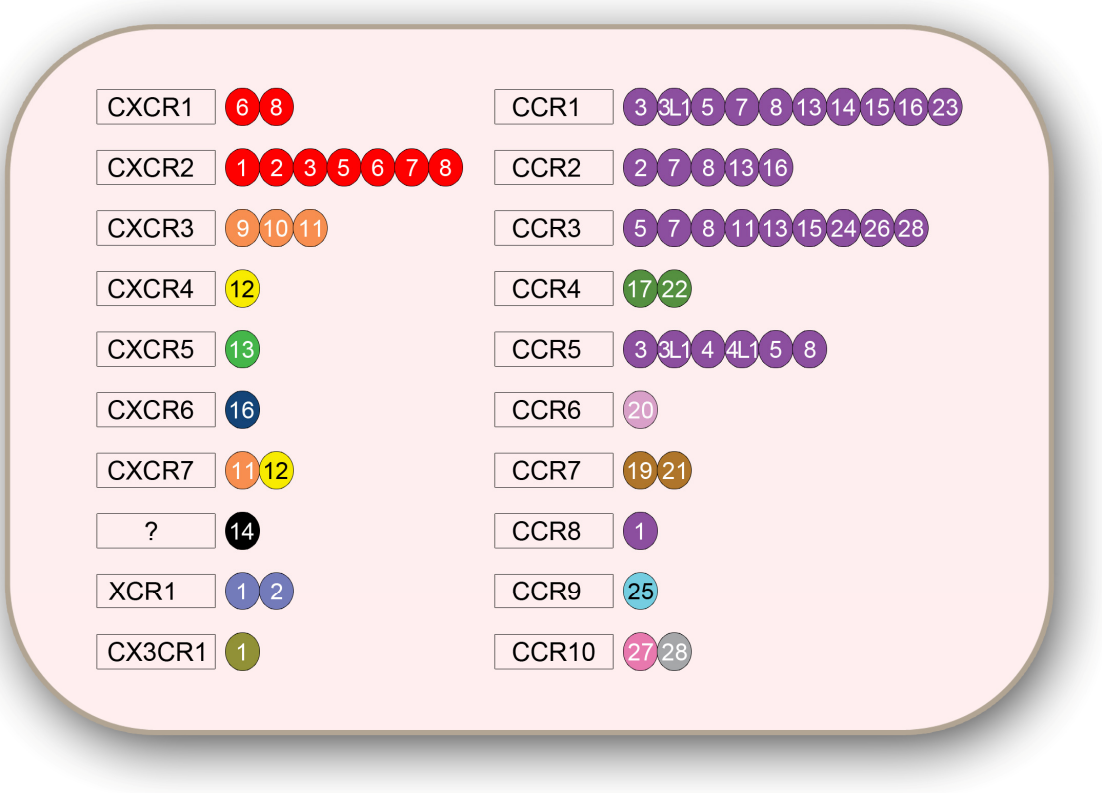

Figure 2.3 Chemokine superfamily arranged by the receptors they bind to. Chemokines are represented by only their ligand number. The receptor name also indicates whether each ligand is a CC or CXC. Colors represent the chromosomal location of the ligands: the genes encoding the ligands shown in the same color are at the same chromosomal location. Ligands whose genes are located in the same chromosomal location tend to bind to the same receptor. Adapted and modified from (ZlotnikYoshie & Nomiyama 2006).

2.8 Antimicrobial peptides

Although the *Stratum corneum* represents the first line of protection against the invasion by microbial agents this physical barrier is susceptible to injuries allowing the entry of opportunistic microbial agents into the skin.

The innate immune system can immediately react to this intrusion helping to prevent further invasion. This immune response includes phagocytosis by neutrophils and macrophages and their production of reactive oxygen intermediates that kill microbial agents (Fearon & Locksley 1996).

A number of endogenous antimicrobial peptides constitute a major component of the in innate immunity (LehrerLichtenstein & Ganz 1993). In order to exert their antimicrobial effects these peptides adhere to and permeabilize the surface membranes of potential pathogens. This activity is a consequence of

several common features such as a high content of basic residues and the tendency of some to adopt an amphipathic conformation (Hancock & Rozek 2002, JenssenHamill & Hancock 2006).
There are two major groups of human antimicrobial peptides in the skin: the human β-defensins (HBDs) (Harder *et al.* 1997, Stolzenberg *et al.* 1997) on the one and the cathelicidins (Frohm *et al.* 1997, Gallo *et al.* 1994) on the other hand. These peptides are produced by keratinocytes (Fulton *et al.* 1997) and have antimicrobial activity against bacterial, fungal, and viral pathogens (Gropp *et al.* 1999).

2.8.1 Defensins

Defensins are positively charged, single chain peptides with a molecular weight of 3.0 to 4.5 kDa that can be classified into the α- and β-defensin subfamilies based on the pairing of cysteines in three disulphide bridges. Six α-defensins and four β-defensins have been previously identified in humans (Bals 2000). HBDs are expressed mainly in epithelial cells. While HBD1 is generally constitutively expressed (ZhaoWang & Lehrer 1996) the expression of HBD3 can be increased by injury or by inflammation of the skin (Harder *et al.* 2001). HBD3 was discovered by isolation from human lesional psoriatic scales. It demonstrates a broad spectrum of potent antimicrobial activity against many potentially pathogenic microbes including multiresistant *S. aureus* and vancomycin-resistant *Enterococcus faecium*. Proinflammatory cytokines like TNF-α and IL-1β and contact with bacteria have been found to induce HBD3 mRNA expression in keratinocytes (Harder et al. 2001).

2.8.2 Cathelicidins

Cathelicidins are defined by a highly conserved N-terminal structural cathelin domain and a structurally variable cationic antimicrobial peptide at the C-terminus. The human cathelicidin gene CAMP encodes an inactive precursor LL37/human cationic protein 18 kDa (hCAP18), which is expressed and stored in neutrophils. It requires additional processing by proteinase 3 to yield its C-terminal antimicrobial peptide, LL37 (Agerberth *et al.* 1995, Sorensen *et al.* 2001). Its expression in keratinocytes can be induced by injury or inflammation

of the skin. *In vitro* LL37 shows a broad-spectrum antimicrobial activity against several potentially pathogenic gram-negative and gram-positive bacteria at mM concentrations. The *in vivo* relevance of cathelicidins in cutaneous host defense has been demonstrated in a mouse model. Mice deficient in the expression of the mouse homolog cathelicidin CRAMP (cathelin-related antimicrobial peptide) were more susceptible to *group A streptococcal* skin infection (Nizet *et al.* 2001).

3 Aim of the thesis

This thesis was aimed to characterize the underlying molecular and cellular mechanisms of EGFR-I associated adverse events during targeted cancer therapy. Based on these findings novel rational-based strategies for the management of EGFR-I associated cutaneous adverse events should be developed.

4 Material & Methods

4.1 Buffers and solutions

PBS (phosphate buffer saline), 20 x	160 g NaCl 4 g KCl 28.8 g Na_2HPO_4 + 2 H_2O 4.8 g KH_2PO_4 ad 1000 ml ddH_2O	adjust to pH 7.4
C-buffer	1 mg bovine serum albumin (BSA) 1 ml 4-(2-hydroxyethyl)-1-piperazineethanesulfonic acid (HEPES) ad 100 ml RPMI 1640	
Ammonium chloride lysis buffer	8.29 g NH_4Cl 1 g $KHCO_3$ 0.0375 g Na_2-EDTA ad 1000 ml ddH_2O	adjust to pH 7.4
Protein lysis buffer	50 mM HEPES pH7.4 150 mM NaCl 1% NP40 0.1% SDS 1% Triton X-100	
MOPS buffer	83.7 g MOPS 13.6 g Sodium Acetate 20 ml 0.5 M EDTA ad 1000 ml ddH_2O	adjust to pH 7

Transfer buffer	2.9 g Glycine 5.8 g Tris-base 3.7 ml 10% SDS 200 ml methanol ad 1000 ml dH_2O	
TBS buffer 10x	24.2 g Tris/HCl 80 g NaCl ad 1000 ml ddH_2O	adjust to pH 7.6
TBS-T Buffer	1 x TBS, 0.1% Tween-20	

Chemical were from Sigma-Aldrich, Saint Louis, MO except as noted.

4.2 Study subjects

The study participants included 107 patients at two centers (Department of Dermatology, University Hospital Duesseldorf, and Department of Dermatology and Allergy, Ludwig-Maximilian University, Munich, Germany). Patients had a mean age of 60 years (range 38 to 87 years) who had been enrolled from March 2007 to October 2009. They had received erlotinib (Tarceva®, Hoffmann-La Roche), the small molecule EGFR tyrosine kinase inhibitor, or cetuximab (Erbitux®, Merck, Darmstadt, Germany), the chimeric monoclonal antibody directed against the EGFR and had consecutively developed papulo-pustular rashes. Patients received EGFR-I due to non-small-cell lung cancer (NSCLC; 50 patients), colon carcinoma (39 patients), squamous-cell carcinoma of the head and neck (HNC; 11 patients), advanced pancreas carcinoma (4 patients), as well as other tumor entities (3 patients) (table 4.1). The rash occurred within 2 to 60 days after therapy initiation but at an average of 11.6 days. In general, patients initially developed papular lesions. Papular lesions then progressed to develop the characteristical pustular aspect in the course. Rash severity was graded according to the National Cancer Institute Common Terminology Criteria

for Adverse Events (CTCAE, version 3.0) as well as to the EGFR-I induced rash severity score (ERSS), a specific scoring system introduced by Wollenberg and co-workers in 2008 (Wollenberg *et al.* 2008). In our collective the rash severity ranged from stages I to III (CTCAE) or 5.3 to 77.9 (ERSS), respectively. The mean ERSS prior to dermatological measures was 42.18. Serum was obtained from 18 patients after obtaining informed consent. Skin biopsies (6mm) were taken after obtaining informed consent from lesional skin of patients treated with erlotinib (lesional) or from healthy individuals undergoing plastic surgery (healthy). Skin samples were either immediately stored in 4% paraformaldehyde (PFA) (Sigma-Aldrich, Saint Louis, MO) or snap-frozen in liquid nitrogen and stored at -80°C. Microbiologic skin swaps were performed in all patients presenting with pustular lesions or signs of skin infection (n=40) and were analyzed by the local institutes for microbiology. The study was approved by the local ethics committees.

Characteristics of the Study Group	
Age (yr)	
Mean:	60.8
Range:	38 - 87
Sex	
Total:	107
Male:female ratio	55:52
Male (%)	58.85
Tumor site (no.)	
Total:	107
Lung:	50
Colon:	39
Head-and-Neck	11
Pancreas:	4
Other:	3
Clinical tumor stage (no.)	
Total:	69
I or II:	4
III:	6

IV:		59
Unknown:		38
Duration to rash occurrence (days after therapy initiation)		
Mean:		11.6
Range:		2 - 60
Rash severity (CTCAE v3.0)		107
Total:		107
I:		16
II:		41
III:		50
IV or V:		-
ERSS (initial admission)		
Mean:		42.18
Range:		5.3 -77.9
Microbial swaps (no.)		40
Bacterial colonization (no.)		
Total:		28 (70%)
Thereof:	*S. aureus*	15 (53.6%)
	Enterobacteriaceae	5 (17.9%)
	Others	8 (28.6%)

Table 4.1 Characterization of the group studied.

4.2.1 Treatment

In order to analyze the efficacy of potential mechanism-based rash-management strategies a retrospective study was conducted. Selection criteria included patients treated with erlotinib or cetuximab that suffered from EGFR-I associated rash at the time of referral. Selection was limited to initial patients and their follow-up visits in the time frame of March 2007 to October 2009. 27 patients were enrolled who presented with an ERSS of 10 or higher. In stage 1, 20 patients were treated topically with mometason furoate cream (Ecural®, Essex Pharma GmbH, Munich, Germany) twice daily for 3 weeks. In stage 2, 23 patients with an ERSS <50 were treated topically with nadifloxacin 1% cream (Nadixa®, Dr. R. Pfleger Chemische Fabrik GmbH, Bamberg, Germany) once daily in the morning in combination with prednicarbate 0.25% cream

(Dermatop®, Sanofi Aventis, Frankfurt, Germany) once daily in the evening for 3 weeks. In stage 3, finally, 4 patients with an ERSS >50 additionally received the systemic retinoid isotretinoin (Aknenormin®, Almirall-Hermal, Barcelona, Spain) 10-20 mg/d for 3 weeks. Rash severity (ERSS) was assessed prior to as well as at the endpoint of therapy.

4.2.2 Assessment of rash severity

Clinical rash severity was assessed applying the National Cancer Institute Common Terminology Criteria for Adverse Events (CTCAE, version 3.0) as well as the ERSS. Briefly, the ERSS-score is a combined skin score of the severity of 5 different aspects of the EGFR-I rash (color of erythema, distribution of erythema, papulation, postulation and scaling/crusts with a balanced score of 0-3 each), the affected facial area, and the total body area involved. The score value may range between 0 (no skin affection) and 100 (maximal skin affection), and is especially sensitive for facial lesions (Wollenberg et al. 2008).

4.3 Cell culture

Primary human keratinocytes were grown in keratinocyte medium (GIBCO, Invitrogen, Carlsbad, CA) supplemented with recombinant EGF (0.1-0.2 ng/ml) and bovine pituitary extract (BPE) (20-30 µg/ml), L-Glutamate (2mM) (PAA, Pasching, Austria) and 1% of a mixture of antibiotics (penicillin 100 U/ml, streptomycin 100 µg/ml) (PAA, Pasching, Austria).
Primary human fibroblasts were grown in fibroblast basal medium (FGM®, Lonza, Basel, Switzerland) supplemented with FGM®-2 SingleQuots® (Lonza, Basel, Switzerland).
Cells were routinely cultured in an incubator at 37°C with 95% humidity and 5% CO_2 (INCO 2, Memmert, Schwabach, Germany).
Erlotinib stock solution (10 mM) (Roche, Basel, Switzerland) was prepared by dissolving 50 mg of Erlotinib (molecular weight (MW): 429.907 g/mol) powder in 11.6 ml DMSO (Sigma-Aldrich, Saint Louis, MO). Aliquots were stored at -20°C. The treatment solutions were freshly diluted using cell specific medium. Usually, cells were treated for 24 h. In particular, mRNA expression analysis of CCL27 was performed after 1 h incubation of erlotinib.

TNF-α (AbD Serotec, Kidlington, UK) and IL-1β (R&D Systems, Inc., Minneapolis, MN) were diluted in the treatment solutions to a concentration of 10 ng/ml and 5 ng/ml, respectively.
PD-98059 (Biomol, Enzo Life Sciences International, Inc., Plymouth Meeting, PA) is a potent and selective inhibitor of MAP kinase kinase (MEK). It selectively blocks the activation of MEK thereby inhibiting the phosphorylation and the activation of MAP kinase. The stock solution (5 µM in DMSO) was diluted to a concentration of 5 nM in keratinocyte media.
SP600125 (Biomol, Enzo Life Sciences International, Inc., Plymouth Meeting, PA) inhibits the phosphorylation of c-Jun (JNK inhibitor). The stock solution (20 mM in DMSO) was diluted to a concentration of 20 µM in keratinocyte media.

4.4 Cutaneous wound healing assay

For wound healing assay analysis cells were cultured in 6-well plates until confluency. Cells were treated with appropriate treatment solutions and subsequently, the monolayer of cells was scratched across each well using a fine pipette tip in order to create a cell-free area. This was set as time point zero (t=0). Images of the same area were taken under bright field at t=0 and after an incubation time of 12 h. The widths of the wound scratches at different time points were measured and expressed as a percentage of the initial distance at t=0.

4.5 Immunohistochemistry

4.5.1 Tissue embedding

Skin biopsies were immediately snap frozen in liquid nitrogen and stored at -80°C upon dissection. Before processing they were either embedded in Tissue-Tek® O.C.T. compound (Sakura, Zoeterwoude, Netherlands) or fixated in 4% formaldehyde-solution (Otto Fischar GmbH & Co. KG, Saarbrücken) for paraffin embedding.

4.5.2 Tissue sectioning

Tissue samples were cut into 5 µm (formalin) or 9 µm (frozen sections) transversal sections by use of either a microtome (1150/Autocut, Reichert-Jung, Wetzlar, Germany) or cryomicrotome (-30°C) (2800 Figocut E, Reichert-Jung, Wetzlar, Germany), and subsequently mounted on adhesive microscope slides (Thermo Scientific, Waltham, MA). Paraffin embedded sections were stored at RT. Cryoprotected slides were stored at -80°C.

4.5.3 Histochemical staining

All stainings were carried out according to the following general protocol. Minor modifications depending on the antibody were applied (table 4.2). All antisera and antibodies were diluted in PBS. Antibody specificity controls included replacement of primary antibodies by specific isotype controls (table 4.2).
Paraffin embedded sections were deparaffinized in xylene (Merck, Darmstadt, Germany) and rehydrated in decreasing series of ethanol (Merck, Darmstadt, Germany). Sections were finally washed in PBS. Frozen sections were air dried and postfixed for 10 min in acetone (Roth, Karlsruhe, Germany) or 4% PFA (Sigma-Aldrich, Saint Louis, MO).
Endogenous peroxidases were quenched by treatment with 1% H_2O_2 in methanol (Merck, Darmstadt, Germany) for 10 min. In order to block non-specific binding sites sections were incubated for 30 min in 2% normal horse serum (Pan Biotech, Aidenbach, Germany) at RT. The diluted primary antibody (table 4.2) was applied onto sections after normal horse serum had been drained off.
After incubation of the primary antibody sections were washed in PBS. Immunoreactions were detected with species-specific biotinylated secondary antibodies (Vector Laboratories, Inc., Burlingame, CA). Slides were rinsed in PBS in order to remove unbound antibody, and subsequently incubated in streptavidin horseradish peroxidase-(HRP) conjugate (Dako, Glostrup, Denmark). Bound antibody was visualized using the Elite-ABC reagent (Vector Laboratories, Inc., Burlingame, CA) with 3-Amino-9-Ethyl-carbazol (AEC) (Vector Laboratories, Inc., Burlingame, CA) as a substrate according to the manufacturer's instructions. Following washes slides were counterstained with

hematoxylin (Sigma-Aldrich, Saint Louis, MO) and eosin (Roth, Karlsruhe, Germany) for less than 1 min at RT, rinsed in water, and permanently mounted in Ultramount Plus (Labvision Products, Fremont, CA). Immunoreactions were detected by use of a microscope (Axiovert 200M) (Zeiss, Jena, Germany) using Axiovision 4.7 (Zeiss, Jena, Germany). Analyzes were performed using and ImageJ Software (Bethesda, MD).

Primary Antibody	Dilution / Incubation time	Company
Monoclonal mouse anti-human EGFR, DAK-H1-WT, $IgG_1\kappa$	7 µg/ml (1:50) , 90 min at 37°C	Dako, Glostrup, Denmark
Monoclonal mouse anti human p-EGFR Tyr1068 (1H12), IgG_1	1:100 PBS/0.1% Triton® X-100, o.n. 4°C	Cell Signaling Technology, Beverly, MA
Monoclonal mouse anti-human Erk, 16/ERK (pan ERK), IgG_{2a}	2.5 µg/ml, 1:100 PBS/0.1% Triton® X-100, 2 h RT	BD Bioscience, San Jose, CA
Monoclonal mouse anti-human p-Erk (E-4), IgG_{2a}	2 µg/ml, 1:100 PBS/0.1% Triton® X-100, 2h RT	Santa Cruz Biotechnology, Inc., Santa Cruz, CA
Monoclonal mouse anti-human CD1a, NA1/34, $IgG_{2a}\kappa$	1:100, 2 h RT	Dako, Glostrup, Denmark
Monoclonal mouse anti-human CD68, KP1, $IgG_1\kappa$	5 µg/ml, 2 h RT	Dako, Glostrup, Denmark
Monoclonal mouse anti-human CD4, 4B12, $IgG_1\kappa$	5 µg/ml, 2 h RT	Dako, Glostrup, Denmark
Monoclonal mouse anti-human CD8, CD8/144B, $IgG_1\kappa$	2.5 µg/ml, 2 h RT	Dako, Glostrup, Denmark
Monoclonal mouse anti-human Neutrophilic Elastase, NP57, $IgG_1\kappa$	1 µg/ml, 45 min RT	Dako, Glostrup, Denmark
Monoclonal mouse anti-human CCL27, 124302, IgG_{2a}	20 µg/ml, 2 h RT	R&D Systems, Inc., Minneapolis, MN
Monoclonal mouse anti-human CXCL14, 131120, IgG_{2a}	20 µg/ml, o.n. 4°C	R&D Systems, Inc., Minneapolis, MN
Polyclonal goat anti-human CCL5, (C-19), IgG	20 µg/ml, 110 min 37°C	Santa Cruz Biotechnology, Inc., Santa Cruz, CA
Monoclonal mouse anti-human Mastcell Tryptase, AA1, $IgG_1\kappa$	15 µg/ml, 90 min 37°C	Dako, Glostrup, Denmark

Isotype control $IgG_1κ$		BD Bioscience, San Jose, CA
Isotype control $IgG_{2a}κ$		BD Bioscience, San Jose, CA
Isotype control normal goat IgG		Santa Cruz Biotechnology, Inc., Santa Cruz, CA

Table 4.2 List of different primary antibodies, isotype controls and corresponding dilutions.

4.6 Transwell migration assay

Migration assays were performed by using Costar® 24-transwell chemotaxis chambers (Corning Costar Corporation, Corning, NY) with 3.0 µm pore size polycarbonate filters (Corning Costar Corporation, Corning, NY).
In brief, 300 µl of supernatant of erlotinib co-stimulated (TNF-α, IL-1β) primary human keratinocytes and 300 µl of chemotaxis buffer (C-buffer) was placed in the lower well which was previously coated with Sigma Coat (Sigma-Aldrich, Saint Louis, MO). The upper filters of the chemotactic chambers were loaded with 100 µl of cell suspension of isolated T cells at a concentration of 1×10^6 cells/ml. Each condition was set up in triplicates. Undiluted chemotaxis buffer was used as in internal negative control. Plates were kept at 37°C for 3 h. Thereafter, the suspension of cells which migrated to the lower wells through the filters was then collected in 5 ml round bottom tubes (BD Biosciences, San Jose, CA) for further analysis.
The percent of migrating cells was determined by dividing the number of cells migrated in the experimental condition by the number of total cells (cells only without filters).

4.7 T cell isolation

"Buffy coats" are concentrated suspensions of lymphocytes obtained during procession of total blood. Peripheral blood mononuclear cells (PBMCs) can be isolated from buffy coats by Ficoll density-gradient centrifugation. Lymphocytes and monocytes will concentrate at the interphase between the upper phase (plasma, thrombocytes) and the lower phase (Ficoll) according to their specific density. Erythrocytes and granulocytes of higher density will form a cell pellet.

Briefly, the buffy coat cell suspension was diluted 1:2 with RPMI 1640 (Lonza, Basel, Switzerland). 37.5 ml of cell suspension was layered on top of 12.5 ml Ficoll-Paque^{TM} Plus solution (GE Healthcare, Buckinghamshire, UK) and was separated by centrifugation (1150 rpm, 20 min, RT) (Rotina 46 R, Hettich, Bäch, Switzerland) without break. The interphase, containing the PBMC, was carefully transferred into a fresh tube, washed in RPMI 1640 (GIBCO, Invitrogen, Carlsbad, CA), and centrifuged again. The resulting pellet was resuspended in 25 ml of ammonium chloride lysing buffer to lyse erythrocytes and incubated for 10 min at 4°C. Thereafter, the remaining cells were washed in PBS (GIBCO, Invitrogen, Carlsbad, CA), and subsequently centrifuged (1150 rpm, 10 min, 8°C).

The cells were then resuspended in RPMI 1640. Depletion of monocytes and macrophages was carried out in 175 cm^2 cell culture flasks (Greiner Bio-One GmbH, Kremsmünster, Austria) at standard cell culture conditions as monocytes and macrophages will adhere to the wall of the plastic flask. Therefore the non adherend cells were suspended in 20 ml of RPMI 1640, centrifugated as above, and resuspended in 4 ml of 1 x column wash buffer (R&D Systems, Inc., Minneapolis, MN). T cell isolation was performed by the use of human T cell enrichment columns (R&D Systems, Inc., Minneapolis, MN) according to the manufacturer's instructions. Finally, T cells were resuspended in appropriate medium or chemotaxis buffer.

4.8 Flow cytometry analysis

Lymphocyte subset analysis was done on FACS Calibur flowcytometer (BD Biosciences, San Jose, CA) using CellQuest software (BD Biosciences, San Jose, CA) and visualized in a histogram plot (counts over fluorescence). In each of the tube at least 50,000 events were counted. Therefore a fixed amount of beads (Polymer Microspheres) (Bangs Laboratries, Inc., Fishers, IN) was added to the samples.

Flow cytometric analysis was performed using fluorescein isothiocyanate- (FITC), R-phycoerythrin- (R-PE), and PE-Cy5-conjugated monoclonal antibodies (mAbs) to human CLA, CD8 and CD4 (all from BD Biosciences, San Jose, CA), respectively.

Cells were blocked with AB-type human Serum (heat-inactivated) (Pel-Freez Biologicals, Rogers) and horse serum (Biochrom AG, Berlin, Germany), and were then incubated with the mAbs for 45 min at 4°C. Cells were washed with PBS, centrifugated (Rotixa/RP, Hettich, Bäch, Switzerland) and resuspended. Finally, cells were fixed with 1% paraformaldehyde (Sigma-Aldrich, Saint Louis, MO) in PBS (PAA, Pasching, Austria) and kept in the dark.
FITC- (rat IgM), R-PE- (IgG_1), and PE-Cy5- (IgG_1) conjugated isotype controls (all from BD Biosciences, San Jose, CA) were used to determine non specific staining. Cells were initially gated on the basis of forward scatter (FSC) and side scatter (SSC) characteristics with gates set to remove dead cells.

4.9 Western Blot analysis

For western blot analysis a sodium dodecyl sulfate-polyacrylamide gel electrophoresis (SDS-PAGE) was realized to separate the proteins by size which was then transferred from the gel to a membrane via electro transfer. Finally, this blot was processed for the detection of specific proteins with a primary antibody detected by a chemifluorescent secondary antibody.

4.9.1 Protein lysates

Cells were washed with ice cold PBS on ice and 150 µl of the protein lysis buffer containing protease inhibitor cocktail III (1:1000, Calbiochem, Merck, Darmstadt, Germany) and phosphatase inhibitor V (1:50, Calbiochem, Merck, Darmstadt, Germany) was added to cells. They were incubated on ice for 5 min before cells were scraped from each well and transferred to 1.5 ml tubes. After cells were centrifuged for (10 min, 13000 rpm, 4°C) (Eppendorf Centrifuge 5415C) the supernatant was removed and analyzed for protein content using the Bradford assay. The protein concentrations of all samples were equalized with sample buffer.

4.9.2 Protein measurements

Protein concentration was determined according to Bradford (Bradford 1976). For each sample 200 µl of Bradford protein reagent (Bio-Rad Laboratories Inc.,

Hercules, CA) was added to 800 µl of water (dH_2O) without (control) and with protein lysate added. The optical density (OD) was determined at 595 nm (Ultrospec 3000, Pharmacia Biotech, GE Healthcare, Buckinghamshire, UK). Absolute quantification was carried out with an appropriate standard curve of bovine serum albumin (BSA) (Sigma-Aldrich, Saint Louis, MO).

4.9.3 SDS-PAGE Gel Electrophoresis

A minimum of 20 µg of protein in a maximal volume of 16 µl were solubilized in 4 µl Roti®-Load1 (Carl Roth GmbH, Germany) for 5 min at 95°C. Samples were loaded on NuPAGE® 4-12% Bis-Tris gels (Invitrogen, Carlsbad, CA). SeeBlue® Plus2 pre-stained standard molecular weight marker (Invitrogen, Carlsbad, CA) and MagicMark™ XP western protein standard (Invitrogen, Carlsbad, CA) were used as protein standards. Minigels were run in MOPS buffer at 200 V in an electrophoresis system (Novex XCell) (Invitrogen, Carlsbad, CA).

4.9.4 Semi-dry transblotting

After separation of the samples on SDS-PAGE the proteins were transferred to polyvinylidene fluoride (PVDF, 0.45 µm) (Amersham, GE Healthcare, Buckinghamshire, UK) or nitrocellulose (Hybond™ ECL™, Biosciences, GE Healthcare, Buckinghamshire, UK) membranes. Gels were carefully removed and equilibrated in transfer buffer for 10 min. Meanwhile, the PVDF membrane was activated by incubation in methanol (Merck, Darmstadt, Germany) for 1 min followed by incubation in transfer buffer for 10 min. At the same time, blotting paper was soaked in transfer buffer and placed on the lower electrode (anode) of the Semi-Dry SD Transblotter (Bio-Rad Laboratories Inc., Hercules, CA). The membrane and the separating gel were placed between two pieces of moist blotting paper. A glass pipette was scrolled over to remove air bubbles between them. Thereafter, the sandwich was covered with the upper electrode (cathode) and blotted at 15 V for 40-45 min.

4.9.5 Immunodetection

Following protein transfer, the membrane was incubated in blocking solution (5% (w/v) non-fat dry milk powder (Sigma-Aldrich, Saint Louis, MO) dissolved in TBS-T buffer) for 30 min, while gently rocking at RT. Primary and secondary antibodies were diluted in blocking solution containing 1% (w/v) milk powder (Sigma-Aldrich, Saint Louis, MO) to the appropriate concentrations (Table 4.3). Incubation with the first antibody was performed overnight at 4°C while gentle shaking. The next day, the blots were washed (3 x 5 min) in TBS-T and incubated with species specific streptavidin HRP-conjugated secondary antibodies (1:10,000) (Amersham Biosciences, GE Healthcare, Buckinghamshire, UK) for 1 h at RT. Following three washes the blots were immersed in enhanced chemiluminescence solution (ECL) (Amersham Biosciences, GE Healthcare, Buckinghamshire, UK) for 2 min and were covered with a plastic bag. The blots were exposed to X-ray film (Amersham Hyperfilm ECL) (Amersham Biosciences, GE Healthcare, Buckinghamshire, UK) for different exposing times. The X-ray films were developed in a dark room with standard reagents (developer and fixer) and dried with warm air.

Primary antibody	Dilution / Incubation time	Company
monoclonal mouse anti-human phospho-EGFR(Tyr1068) (1H12)	1:1000, o.n. 4°C	Cell Signaling Technology, Beverly, MA
rabbit anti-human EGFR (C74B9)	1:1000, o.n. 4°C	Cell Signaling Technology, Beverly, MA
rabbit anti-human phospho-p44/42 MAPK (Erk1/2) (Thr202/Tyr204)	1:1000, o.n. 4°C	Cell Signaling Technology, Beverly, MA
rabbit anti-human p44/42 MAPK (Erk1/2)	1:1000, o.n. 4°C	Cell Signaling Technology, Beverly, MA

Table 4.3 List of different primary antibodies and corresponding dilutions.

4.10 ELISA

Chemokine concentrations in the supernatants of erlotinib stimulated human keratinocytes were measured an enzyme-linked immunosorbent assay (ELISA DuoSet, R&D Systems, Minneapolis, MN) according to the manufacturer's instructions. Briefly, monoclonal capture antibody (2 µg/ml) was incubated overnight in the wells of an immunosorbent 96-well plate (NUNC, Rochester, NY). After blocking with reagent diluents (1% BSA in PBS) for 1 h at RT, wells were aspirated and rinsed with wash buffer (0.05% Tween® 20 in PBS). Samples were then incubated for 2 h. Following another aspiration and wash step, biotinylated detection antibodies (75 ng/ml for CCL27, 250 ng/ml for CXCL14) were incubated for 2 h. After another aspiration and wash step, streptavidin-HRP was incubated in the wells for 20 min. Following a final aspiration and wash step, substrate solution was incubated in the wells for 20 min. Finally, stop solution was added. Optical densities were measured at 450 nm by use of a microplate reader (MR 5000, Dynatech Laboratories, Inc., Alexandria, Va.). Sample concentrations were calculated against standard curves.
For absolute quantification the concentration of protein was determined:

$$x = \frac{\text{OD value} - b}{m}.$$

Where b = y – intercept of the standard curve and m = slope of the standard curve line.

4.11 EMSA (Electrophoretic Mobility Shift Assay)

4.11.1 Preparation of nuclear extracts

Briefly, cells were washed with ice-cold PBS buffer and harvested by adding 500 µl of buffer A (20 mM HEPES, pH 7.9; 10 mM NaCl, 0.2 mM EDTA; 2 mM DTT) containing protease inhibitor and subsequently incubated on ice for

10 min. The supernatant was taken as the cytoplasmic lysate after centrifugation at 14.000 rpm for 3 min. The pellet was resuspended in 50 µl of buffer B (20 mM HEPES, pH 7.9; 420 mM NaCl, 0.2 mM EDTA; 2 mM DTT; 1 mM Na_3VO_4, 25% glycerol) containing protease inhibitor, incubated for 20 min at 4°C and then centrifuged at 14000 rpm for 3 min. The supernatant was collected as nuclear lysate without disturbing the pellet and stored at -20°C until use.

4.11.2 Gel shift

Specific oligonucleotides for binding of AP-1 (59-CGCTTGATGACTCAGCCGGAA) (Santa Cruz Biotechnology, Inc., Santa Cruz, CA) were prepared by end labeling of the 59-terminus with [γ-^{32}P] ATP (Hartmann analytic GmbH, Braunschweig, Germany) in the presence of T4 polynucleotide kinase (Genecraft, Cologne, Germany) and purified by the QIAquick Purification kit (Qiagen, Hilden, Germany). Reactions were performed by incubation of 4 µg nuclear extract with [γ-^{32}P]-labeled oligonucleotide for 30 min at RT in a buffer containing 10 mM Tris, pH 7.5; 50 mM NaCl, 1 mM EDTA; 1 mM $MgCl_2$; 0.5 mM DTT; and 4% glycerol. The specificity of binding was analyzed by competition with unlabeled oligonucleotides. The DNA-protein complexes were then separated on 4% native polyacrylamide gel at 100 V for 2 h, the gels were dried and exposed for autoradiography on X-ray films (Kodak, Rochester, NY).

4.12 Total RNA isolation

RNA extraction was realized from cells by using the TRIzol® Reagent, a monophasic solution of phenol and guanidine isothiocyanate. In fact, this reagent is lysing the cells. Addition of chloroform separates the organic and aqueous (containing RNA) phases. Phenol removes the proteins from nucleic acid samples during isolation.

Briefly, to lyse cells 1 ml of TRIzol® Reagent (Invitrogen, Carlsbad, CA) was added to 1 well of a 6-well plate. After adding 1/5 volume chloroform (Merck, Darmstadt, Germany), cells were vortexed and subsequently centrifuged (15 min, 12000 rpm, 4°C) (Biofuge 13R, Heraeus Sepatech GmbH, Osterode,

Germany). Following centrifugation, the aqueous upper phase was transferred into a new tube and RNA precipitation was achieved by adding ½ volume isopropyl alcohol (Merck, Darmstadt, Germany). The solution was mixed by vortexing, incubated overnight at -20°C, and finally centrifugated (12000 rpm, 30 min, 4°C). The RNA precipitate was visible as a pellet on the bottom and on the side of the tube. To remove any residual salt the pellet was washed in 1 ml of 80% ethanol (Merck, Darmstadt, Germany) after supernatant had been carefully removed. Again the sample was centrifugated for (12000 rpm, 30 min, 4°C). After removal of supernatant, the pellet was dried for 10 min at RT and subsequently dissolved in 50 µl H_2O (DEPC) (Roth, Karlsruhe, Germany). Samples were stored at -80°C.

4.13 OD Measurement

RNA yield was determined using NanoDrop™ 2000 (Thermo Scientific, Wilmington, DE) photometer. RNA concentration was measured according to the manufacturer's manual. An OD 260/280 ratio between 1.8 to 2.1 indicated that extracted RNA was devoid of any appreciable protein, salt, or solvent contamination.

4.14 Quantitative PCR (qPCR) analysis

PCR-based analysis was performed to study gene expression of candidate genes. As quantitative PCR is the most sensitive application it was used to quantitate transcription levels of different genes of interest.

4.14.1 Complementary (cDNA) synthesis

cDNA was synthesized from different messenger RNA (mRNA) templates using reverse transcriptase enzyme Superscript II (Invitrogen, Carlsbad, CA).
Since DNA removal is necessary for subsequent applications DNase digestion was performed. Therefore, 4 µg of total RNA was mixed with the following reagents:

1,5 µl	5 x first strand buffer (Invitrogen, Carlsbad, CA)
1 µl	RNasin Plus (40 U/µl, Promega, Madison, WI)
1 µl	DNase I recombinant (Roche, Basel, Switzerland)

RNase-free water was added to a final volume of 16 µl and prepared mixes were incubated for 20 min at 37°C, 10 min at 70°C, and thereafter placed at 4°C.

RNA was primed with a mixture of 1 µl of anchored oligo$(dt)_{12\text{-}18}$ (0.5 µg/µl, Invitrogen, Carlsbad, CA) and 0.4 µl of random hexamer primers (500 µg/ml, Promega, Madison, WI). RNase-free water was added to a final volume of 20 µl and samples were incubated for 10 min at 70°C in order to reduce RNA secondary structures. Then, the following reagents were added for first strand synthesis:

4.5 µl	5 x first strand buffer (Invitrogen, Carlsbad, CA)
1 µl	0.1 M DTT (Invitrogen, Carlsbad, CA)
1 µl	dNTP mix (10 mM, Bioline USA Inc., Taunton, MA)
0.5 µl	RNasin Plus (40 U/µl, Promega, Madison, WI)
1 µl	Superscript II (200 U/µl, Invitrogen, Carlsbad, CA)
30 µl	Total volume (add RNase-free water)

The reaction was gently mixed and after an initial incubation step of 2 min at 42°C for optimal primer annealing cDNA synthesis was carried out for 50 min at 50°C followed by an incubation step of 15 min at 70°C to inactivate the enzyme (Trio-Thermoblock, Biometra, Göttingen, Germany). Thereafter samples were stored at -20°C.

4.14.2 Primer design

Gene specific oligonucleotides for qPCR were either designed on mRNA sequences deduced from GenBank (see table 4.4) or obtained as a TaqMan® Gene Expression Assays by Applied Biosystems.

Gene	System
CCL27	AOD (Hs00171157_m1)
CXCL14	AOD (Hs00171135_m1)
CCL5	SYBR® Green
CXCL8	AOD (Hs00174103_m1)
CCL20	TaqMan®
CCL2	SYBR® Green
CXCL9	SYBR® Green
CXCL10	SYBR® Green
RNase7	TaqMan®
LL37	AOD (Hs01011708_m1)
HBD3	TaqMan®
SCF	AOD (HS00241497_m1)
HYL1	SYBR® Green
HAS2	SYBR® Green
HAS3	SYBR® Green
p21	SYBR® Green
p53	SYBR® Green
IL-6	SYBR® Green
p53	SYBR® Green
IL-6	SYBR® Green

Table 4.4 Oligonucleotides for qPCR. Oligonucleotides were obtained from MWG (Biotech, Ebersberg, Germany) or AOD (Assays on Demand): (Applied Biosystems Inc., Foster City, CA).

4.14.3 Quantitative real time (qPCR) analysis

In order to quantitate differences in mRNA expression qPCR was performed. qPCR consists in “real time” detection of a specific product as quantitation is carried out after each round of amplification by measuring fluorescence emission. SYBR® Green is a fluorescent dye which intercalates into double-stranded DNA. The more abundant the amplification product the higher the fluorescence emission. In order to detect a fluorescent signal during the thermal PCR program, the qPCR device consists of a thermal cycler combined with an optical detector. In an amplification plot the fluorescent signal in logarithmic

scale is plotted against cycle number. When a target cDNA is amplified the resulting amplification curve starts with an initial flat phase as only little PCR product is formed, therefore a low fluorescent signal is detected. The initial phase is followed by a geometric phase due to exponential amplification of PCR product. When reaction reagents are depleted the amplification curve reaches a final plateau.

When a threshold is set intersecting the curve in its geometric phase the resulting crossing point is called C_t-value (threshold cycle).

Genes expressed at higher rates have higher starting copy numbers and, therefore appear earlier during the amplification resulting in lower C_t-values. As an internal standard gene expression analysis of 18S RNA was used since it is expressed at relatively constant levels throughout different cells.

Quantitative PCR was performed using the Applied Biosystem 7000 System and Power SYBR® Green PCR Master Mix or TaqMan® Universal PCR Master Mix (Applied Biosystems Inc., Foster City, CA). For a final reaction volume of 25 µl per well, the following gene specific mixes were prepared.

	Primer forward	**Primer reverse**	**Detection Mix**	**Target Probe**	**cDNA (25ng/µl)**	**dH_2O**
SYBR® Green	2.5 µl [2 µM]*		12.5 µl		10 µl	
TaqMan®	0.6 µl [45 µM]	0.6 µl [45 µM]	12.5 µl	0.75 µl [10 µM]	10 µl	0.55 µl
Eukaryotic 18S rRNA (TaqMan®)	0.15 µl [10 µM]	0.15 µl [10 µM]	12.5 µl	0.15 µl [10 µM]	10 µl	2.05 µl
TaqMan® Gene Expression Assays (Assay on demand)**	1 µl		10 µl		10 µl	

*Primer mix [2 µM]:
20 µl Forward primer [45 µM], 20 µl Reverse primer [45 µm], 410 µl dH_2O
**Final reaction volume: 21 µl

The following PCR program was applied:

temperature	time	
95°C	10 min	
50°C	2 min	40 cycles
60°C	1 min	
95°C	15 s	

In order to prove whether primer-dimer artifacts had affected the reaction in case of SYBR® Green detection a dissociation protocol was always carried out after termination of the PCR program. In this protocol, the temperature is gradually increased to melt the products formed during the PCR reaction. The melting point can be easily detected since the fluorescent signal decreases as DNA double strands separate and therefore intercalated SYBR® Green is released. Different PCR products obtained with the same primer pair should have approximately the same melting point. In fact, different DNA templates primed with a particular primer pair give rise to amplification products of the same size.

All qPCR samples were run in singles and final raw data was exported as .csv files for further statistical analysis in Excel spreadsheets.

For absolute quantification ΔC_t-values were determined:

$$\Delta C_t = 10^5 \cdot 2^{C_{t,control} - C_{t,sample}}.$$

Where $C_{t,control}$ is the C_t-value obtained for the 18S RNA and $C_{t,\ sample}$ is the C_t-value for a specific gene in a specific sample.

Gene expression was illustrated as mean values ± standard deviation.

For absolute quantification, standard curves were established. These calibration curves were based on known concentrations of recombinant plasmid DNA for each gene, respectively.

4.15 Statistics

Data were expressed at mean +/- standard deviation (SD). Statistical significance was assessed by Student's t-test. P-values below 0.05 were considered as statistically significant (*P ≤ .05, **P ≤ .01, ***P ≤ .001).

5 Results

5.1 Inhibition of the EGFR in human primary keratinocytes

Efficacy of the small molecule inhibitor erlotinib was assessed by inhibitor studies in human primary keratinocytes. Erlotinib prevents phosphorylation of the EGFR in a dose-dependent manner (Figure 5.1 A). In addition, erlotinib affects EGFR downstream signaling proteins such as Erk (Figure 5.1 B).

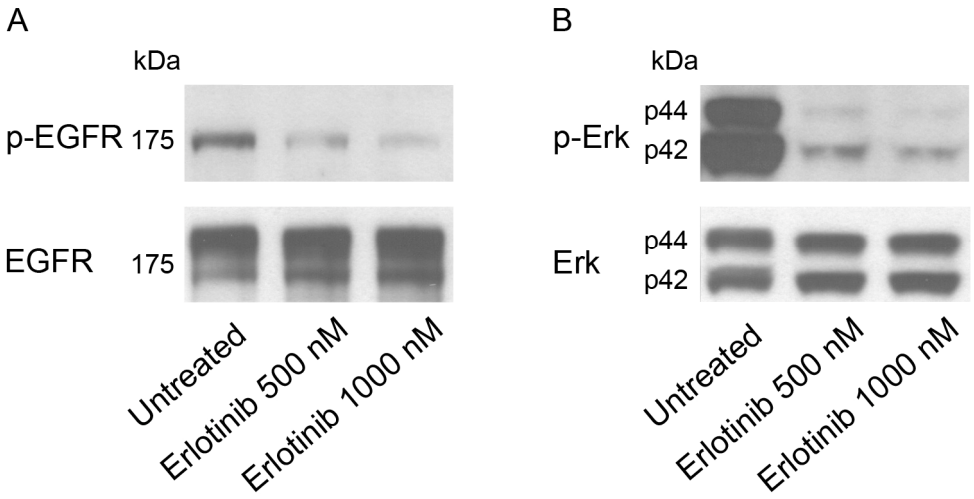

Figure 5.1 Erlotinib dose-dependently inhibits phosphorylation of (A) EGFR and (B) Erk in cultured human primary keratinocytes. Total EGFR and Erk protein is used as an internal control. Shown are representative results of n=3 independent experiments.

5.2 Inhibition of the EGFR in human skin biopsies

In order to validate that EGFR-I induced cutaneous adverse effects are caused by a direct inhibition of EGFR-signaling in the skin rather than through indirect metabolic effects, immunohistochemical analyses were performed. In particular, the level of phosphorylated forms of the EGFR (p-EGFR) and of phosphorylated forms of its downstream-targets Erk1/2 (p-Erk) were determined in skin samples obtained from patients treated with erlotinib. In fact, the expression of p-EGFR

(Figure 5.2 A, B) and p-Erk (Figure 5.2 E, F) is markedly reduced in EGFR-I treated patients as compared to healthy individuals of the same age.

5.3 Characterization of EGFR-I induced skin adverse effects

When patients are treated with EGFR-I, the most frequent and adverse effects are skin toxicities which show signs of inflammation and infection. In fact, more than 50% of the patients are affected with a pruritic papulo-pustular rash (Figure 5.3 A). Histopathological analyses of lesional skin of EGFR-I treated patients reveal a dense, periadnexial inflammatory infiltrate (Figure 5.3 B). This infiltrate is characterized by intraepidermal $CD1a^+$ Langerhans cells (Figure 5.3 C), a marked clustering of $CD68^+$ macrophages (Figure 5.3 D), and T lymphocytes (Figure 5.3 E-G). Notably, quantitative analyses of the infiltrating T lymphocytes demonstrate a significant dominance of $CD4^+$ T helper cells as compared to cytotoxic $CD8^+$ T cells ($P=0.0003$, Student's t-test) or neutrophils (NE) ($P=0.0001$, Student's t-test) (Figure 5.3 H).

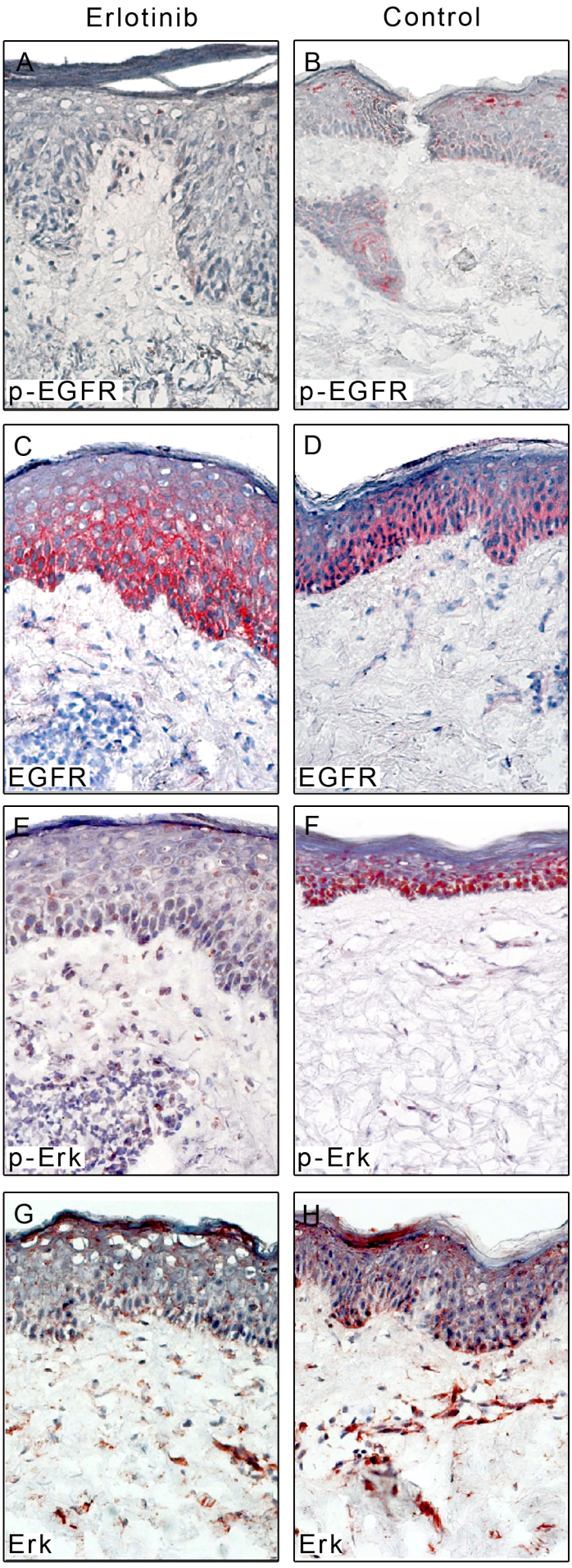

Figure 5.2 Treatment with EGFR-I effectively blocks EGFR-signaling in the skin. Immunohistochemical analysis of (A, B) p-EGFR, (C, D) EGFR, (E, F) p-Erk, and (G, H) Erk expression in skin of healthy individuals (B, D, F, H) and lesional skin of patients (A, C, E, G) treated with erlotinib. Shown are representative results for n=3 individuals.

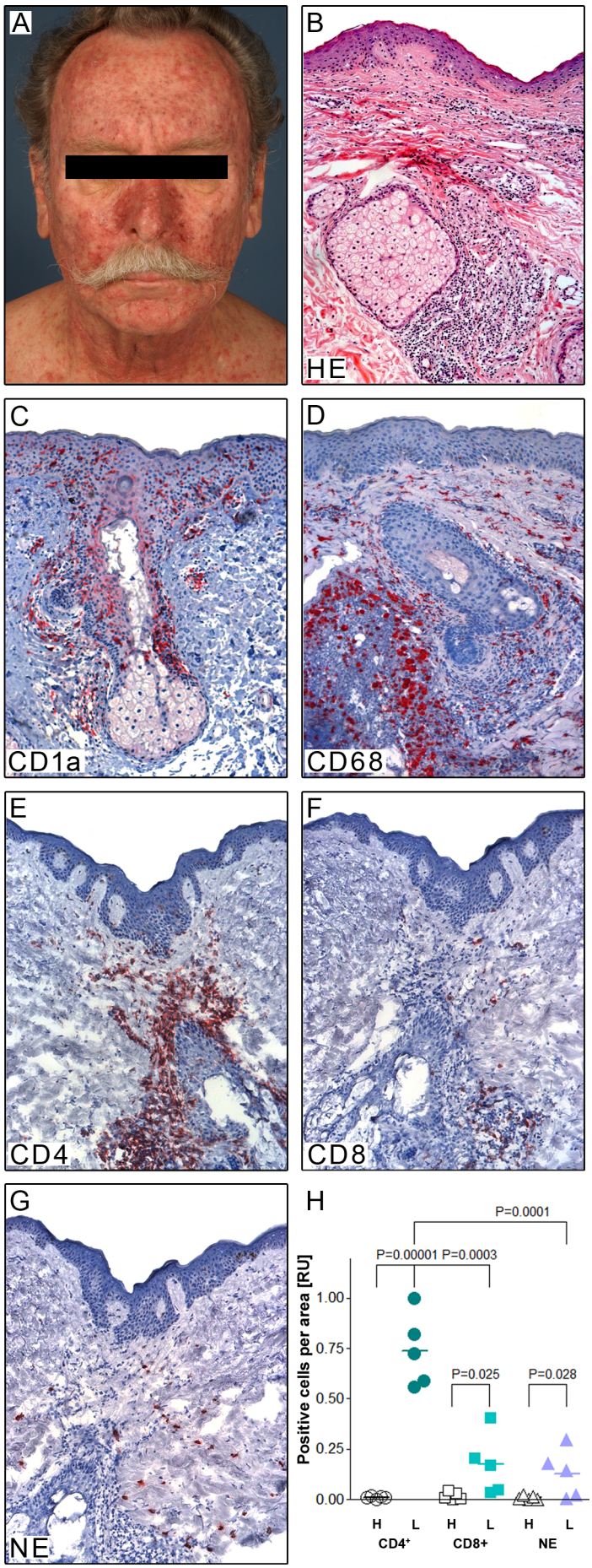

Figure 5.3 Treatment with erlotinib induces skin adverse effects. (A) Characteristical papulo-pustular rash in a 52-year old patient treated with erlotinib. (B) HE staining of lesional skin of a patient treated with erlotinib. Immunohistochemical analysis of $CD1a^+$ (C), $CD68^+$ (D), $CD4^+$ (E), $CD8^+$ (F) and NE^+ (G) cells in the lesional skin of patients treated with erlotinib. (H) Quantitative analysis of immunohistochemistry-based stainings of healthy (H) and lesional (L) individuals (n=5). Values are indicated in relative units of positive cells per area. Statistical analyses are performed using the Student's t-test.

5.4 Chemokine induction in EGFR-I treated keratinocytes

In a next step the molecular and cellular recruitment pathways that direct leukocyte subsets to the sites of EGFR-I induced cutaneous inflammation were analyzed. Therefore, comprehensive analyses of the chemokine expression profile of human primary keratinocytes treated with erlotinib in the presence or absence of pro-inflammatory cytokines (TNF-α, IL-1β) were performed. Notably, different doses of erlotinib significantly induce the expression of pro-inflammatory and skin-associated chemokines such as CCL27, CXCL14, and CCL5 (Figure 5.4.1 A). In contrast, the expression of tumor-associated chemokines, such as CCL20 and CXCL8 is significantly impaired (Figure 5.4.2). In addition, the pro-inflammatory chemokines CCL2, CXCL9, and CXCL10 are also significantly induced following erlotinib treatment (Figure 5.4.2).

After the establishment of a distinct EGFR-I induced chemokine signature in human epidermal keratinocytes *in vitro*, the results were validated *in vivo*. Strikingly, punch biopsies of lesional skin of EGFR-I treated patients reveal a increased chemokine protein expression. Corresponding to the *in vitro* data CCL27, CXCL14, and CCL5 proteins are strongly upregulated in cutaneous lesions of patients treated with erlotinib compared to skin of healthy individuals (Figure 5.4.1 B).

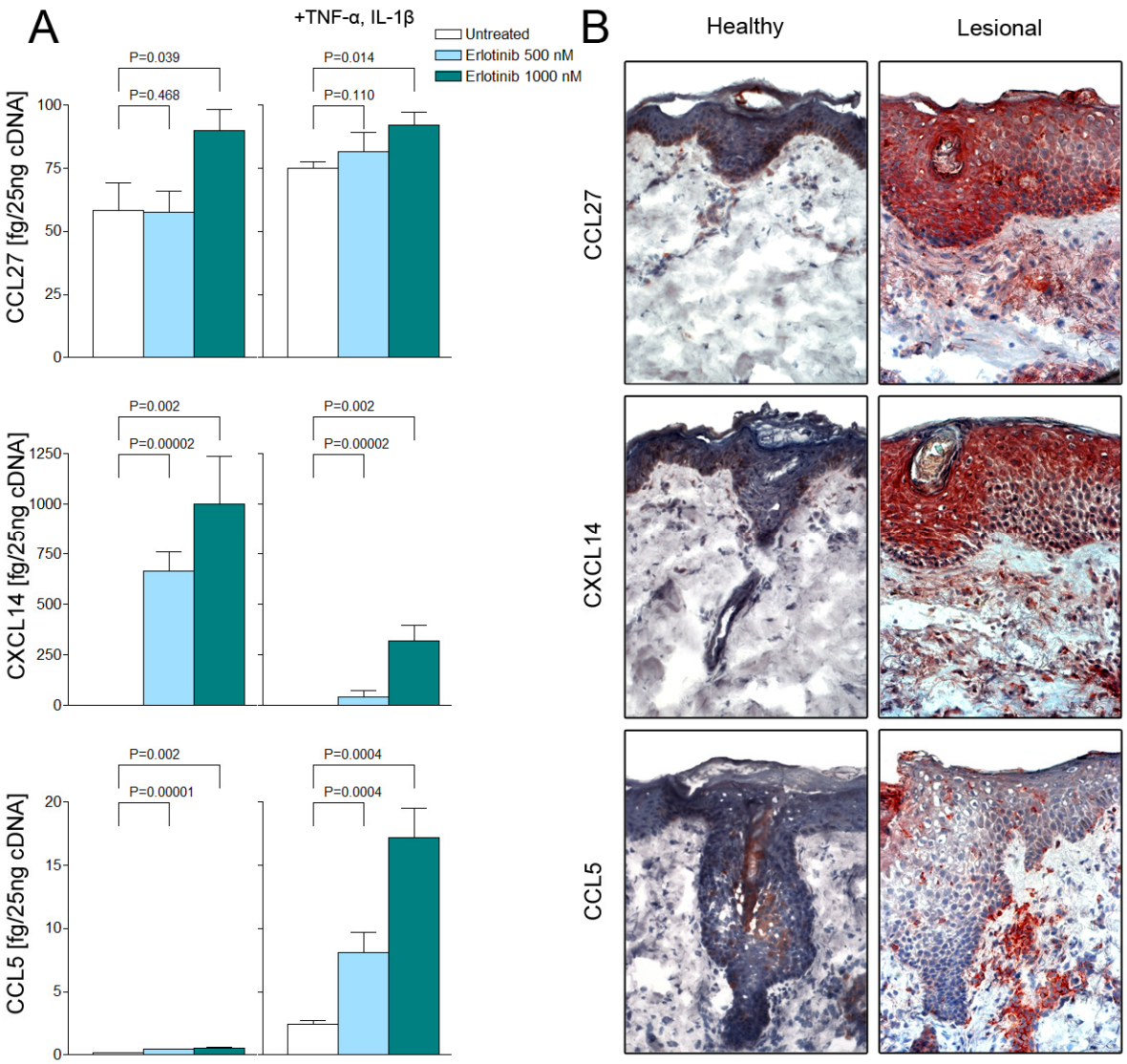

Figure 5.4.1 A set of pro-inflammatory and skin-associated chemokines is upregulated following EGFR-I treatment. (A) In human primary keratinocytes treated with erlotinib and co-stimulated with pro-inflammatory cytokines (TNF-α, IL-1β), the mRNA expression of the pro-inflammatory and skin-associated chemokines CCL27, CXCL14, and CCL5 is significantly induced. Values are expressed as femtograms of target gene per 25 ng cDNA and represent the mean ± SD of three independent experiments (Student's t-test). (B) Lesional skin biopsies of patients treated with erlotinib show strongly induced CCL27, CXCL14, and CCL5 protein as compared to healthy individuals. Shown are representative results for n=3 individuals.

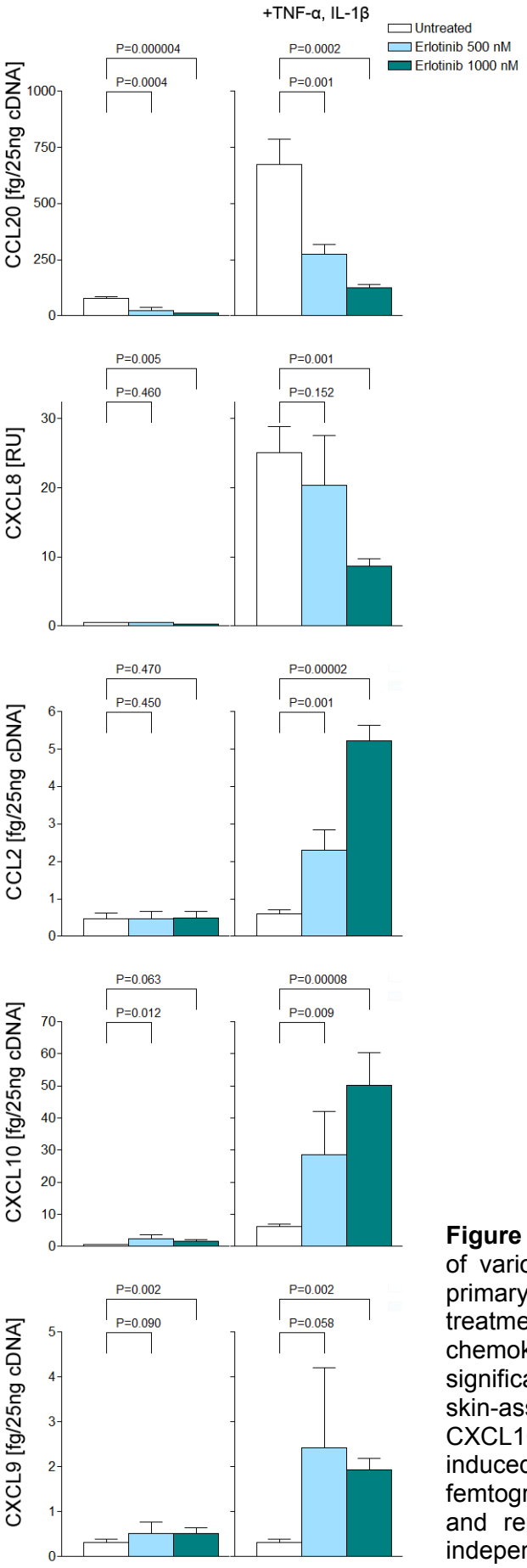

Figure 5.4.2 Quantitative qPCR analyses of various chemokines in cultured human primary keratinocytes following EGFR-I treatment. The tumor associated chemokines CCL20 and CXCL8 show a significant downregulation. In contrast, the skin-associated chemokines CCL2, CXCL10, and CXCL9 are significantly induced. Values are expressed as femtograms of target gene per 25 ng cDNA and represent the mean ± SD of three independent experiments (Student's t-test).

5.5 EGFR-I induced chemokine secretion in keratinocytes

Evaluation of the protein content of CCL27 and CXCL14 in supernatants of EGFR-I treated human primary keratinocytes demonstrate significantly increased concentrations, supporting results of mRNA expression analyses (Figure 5.5 A).

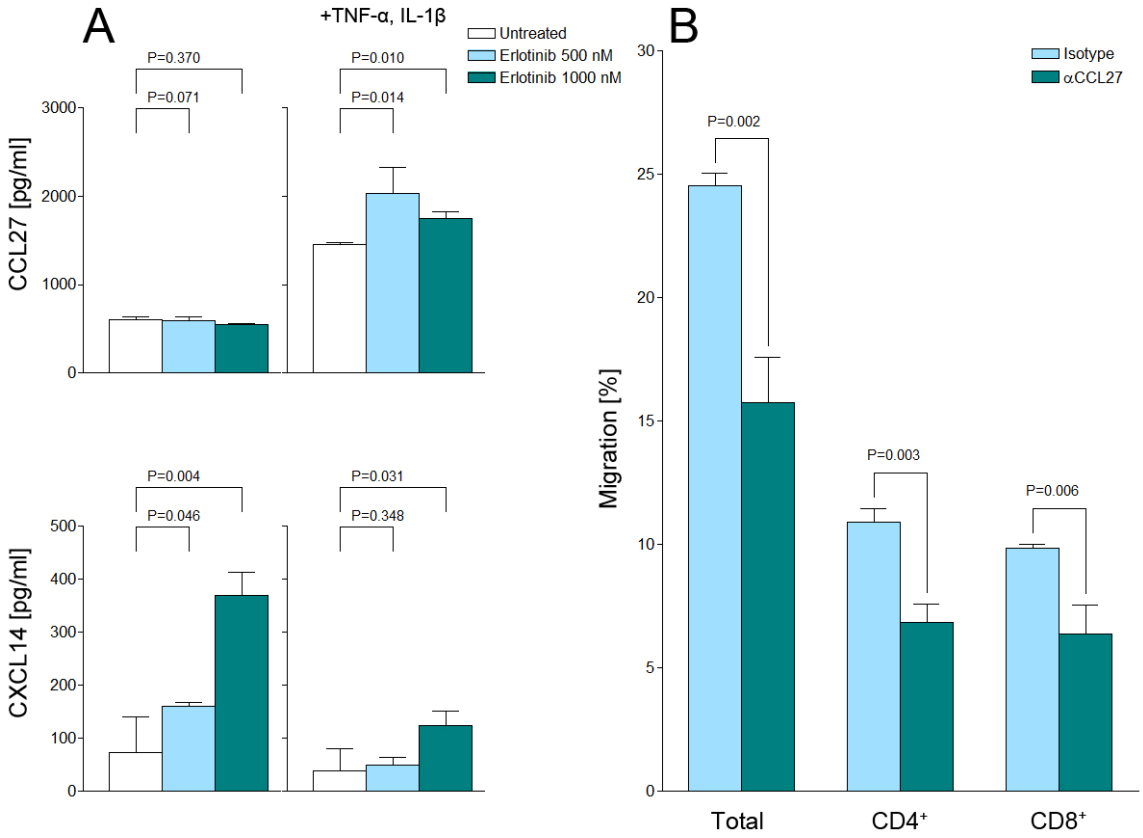

Figure 5.5 EGFR-I significantly induce the production of CXCL14 and CCL27 protein in cultured human primary keratinocytes. CCL27 is functionally active on T cells. (A) CCL27 and CXCL14 protein levels were analyzed in supernatants of erlotinib-treated and co-stimulated (TNF-α, IL-1β) human primary keratinocytes by ELISA. Values are expressed as picograms per ml of media and represent the mean ± SD of three independent experiments (Student's t-test). (B) Transwell chemotaxis assay of T cells (total) and T cell subpopulation ($CD4^+$, $CD8^+$) subjected to supernatants of erlotinib treated human primary keratinocytes supplemented with either isotype control or anti-CCL27 antibody. Migration is expressed as percentage of supplied cells migrating towards the conditioned media. Shown is the mean ± SD of three independent experiments (Student's t-test).

5.6 Chemokine release induces recruitment of T lymphocytes

To investigate the biological relevance of EGFR-I induced chemokine production for T cell recruitment, Transwell chemotaxis assays were performed. Notably, conditioned media of erlotinib-treated primary human keratinocytes have a marked chemotactic effect on total T lymphocytes and T lymphocyte subpopulations as compared to conditioned media of resting keratinocytes (Figure 5.5 B). Strikingly, neutralizing anti-CCL27 antibodies could significantly impair the migratory response of the total T cell population (P=0.002, Student's t-test), CD4+ T cells (P=0.003, Student's t-test) as well as of CD8+ T cells (P=0.006, Student's t-test) (Figure 5.5 B).

5.7 Chemokine induction in EGFR-I human serum samples

Additional examinations of serum samples obtained from patients under erlotinib therapy demonstrate a significant (P=0.00001, Student's t-test) increase in CCL27 protein levels (mean protein concentration = 5025.74 pg/ml) as compared to sera obtained from healthy individuals (mean protein concentration = 692.32 pg/ml) (Figure 5.7). It is noteworthy that CCL27 contents significantly exceed even protein levels observed in the sera of patients suffering from chronic inflammatory skin diseases such as psoriasis vulgaris (PsV) (mean protein concentration = 1137.54 pg/ml) or atopic dermatitis (AD) (mean protein concentration = 3419.79 pg/ml) (Figure 5.7).

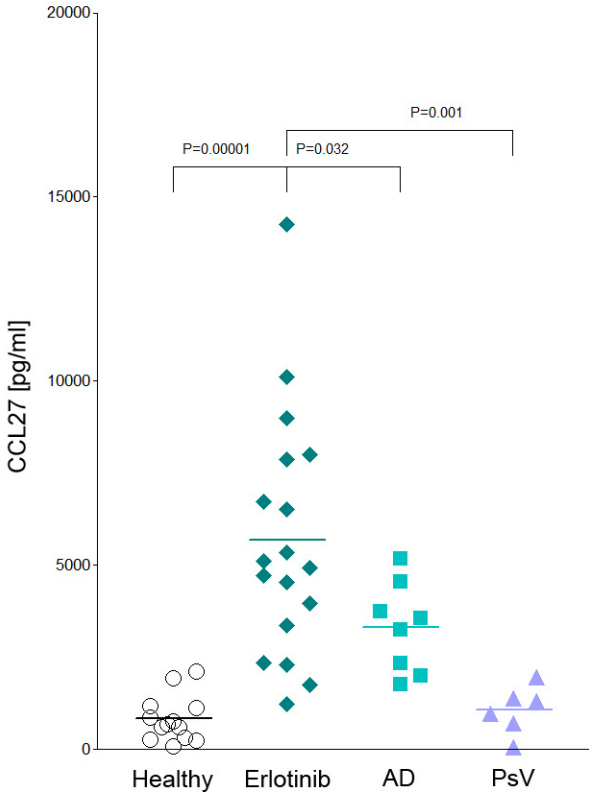

Figure 5.7 Elevated CCL27 protein levels in sera of patients under erlotinib therapy. Results indicate CCL27 protein (pg/ml) expression in sera obtained from healthy individuals (n=12), patients under erlotinib therapy (n=17), atopic dermatitis (AD) patients (n=8) and psoriasis vulgaris (PsV) patients (n=6). Values are expressed as picograms per ml of serum as measured by ELISA. Statistical analyses are performed using the Student's t-test.

5.8 Cutaneous immune defense is affected by EGFR-I

In the present study 70% of microbiological analyses of pustular eruptions or lesions suspicious of infection in patients treated with erlotinib reveal cutaneous bacterial infections or colonizations. Notably, *S. aureus* is detected in the vast majority (53.6%) of the cases and is followed by Enterobacteriacea (17.9%) (Table 4.1).

In order to now elucidate the molecular and cellular mechanisms of the increased susceptibility toward bacterial cutaneous infections in patients treated with EGFR-I, the expression of antimicrobial peptides (AMPs) was evaluated. In particular, expression profiles of the human β-defensin 3 (HBD3), the cathelicidin LL37, the AMP RNase7 were established.

Human primary keratinocytes treated with the EGFR-I erlotinib reveal a significant decrease in AMP expression (Figure 5.8 A). Notably, the expression of RNase7, LL37, and HBD3 is dose-dependently downregulated. Moreover, erlotinib is able to significantly suppress the production of RNase7 protein in cultured human primary keratinocytes (Figure 5.8 B).

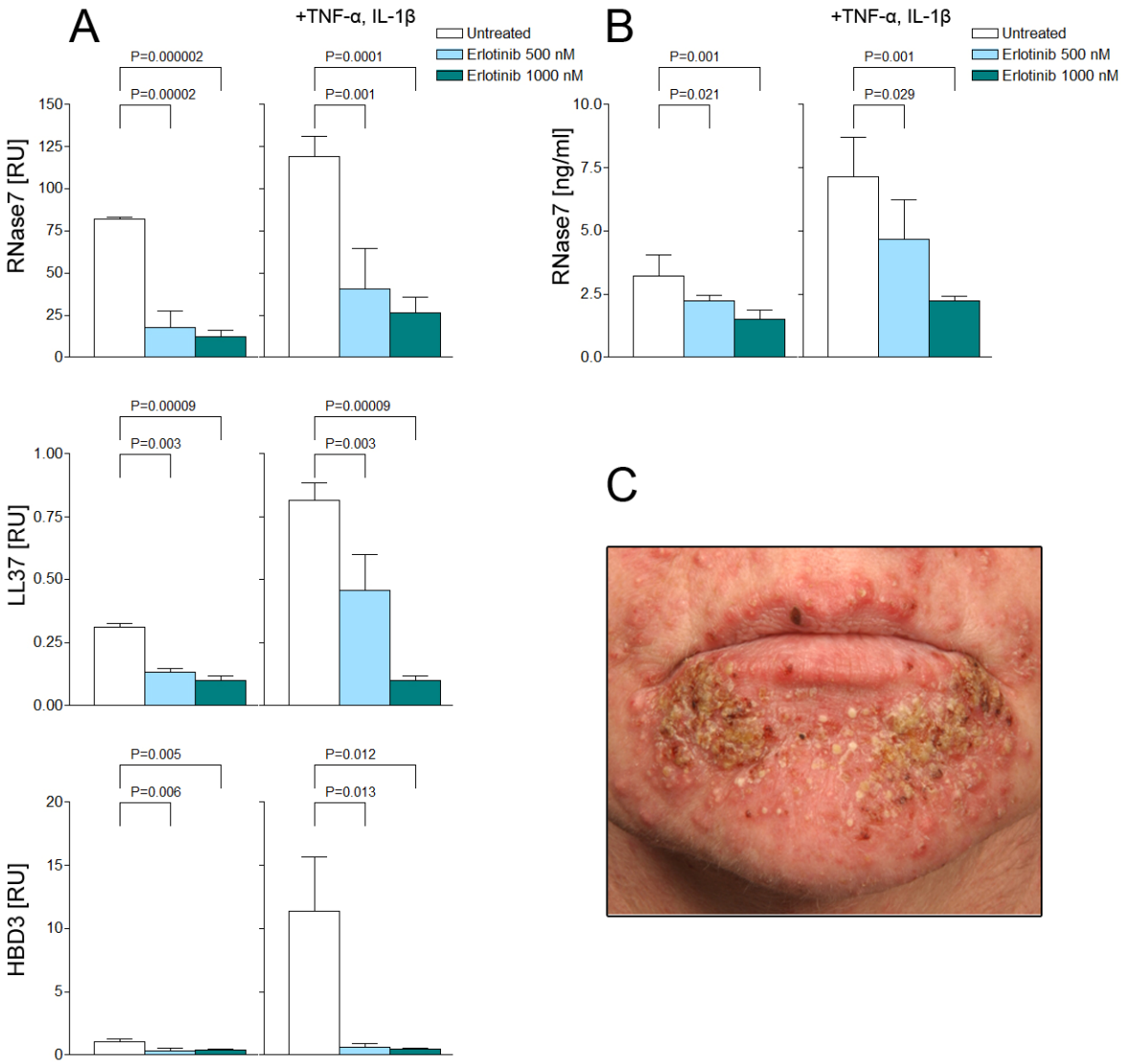

Figure 5.8 EGFR-I impairs the cutaneous immune defense. (A) Quantitative real time qPCR analyses of RNase7, LL37, and HBD3 mRNA in primary human keratinocytes treated with erlotinib in the presence or absence of pro-inflammatory cytokines (TNF-α, IL-1β). Values are expressed as relative units [RU] and represent the mean ± SD of three independent experiments (Student's t-test). (B) RNase7 protein levels in conditioned media of keratinocytes treated with erlotinib and pro-inflammatory cytokines (TNF-α, IL-1β). Values are expressed as picograms per ml of media as measured by ELISA and represent the mean ± SD of three independent experiments (Student's t-test). (C) Clinical presentation of a *S. aureus* superinfection of the rash in an erlotinib-treated patient.

5.9 Molecular mechanisms of EGFR-I mediated CXCL14 production

To further explore the mechanism by which erlotinib induces chemokine expression, particularly CXCL14, a DNA database analysis identified an AP-1 binding site within the putative promoter region of CXCL14. An EMSA assay using radioactively labeled oligonucleotides containing the AP-1 consensus show an increase in AP-1 activity in erlotinib treated primary human keratinocytes compared to untreated cells (Figure 5.9). Furthermore, in addition to erlotinib treatment, primary human keratinocytes were treated with the JNK inhibitor SP600125 (c-Jun-NH_2-kinase) in order to block c-Jun activation. c-Jun is a component of AP-1 and should therefore lead to a decrease in CXCL14 transcription. Indeed, EMSA analysis show that SP600125 lowered AP-1 binding activity (Figure 5.9). In contrast, treating primary human keratinocytes with SP600125 alone did not affect the expression level of AP-1.

To elucidate whether downstream targets of the EGFR pathway can lead to activation of AP-1, an efficient inhibitor of the extracellular signal-regulated kinase (Erk1/2) mitogen-activated protein kinase (MAPK), PD980058, was used in further experiments. Erlotinib treatment in primary keratinocytes results in decreased Erk phosphorylation which indicates that erlotinib not only abrogates EGFR phosphorylation but also effects the expression of downstream molecules (Figure 5.1 B). EMSA analysis of AP-1 in PD98058 treated primary human keratinocytes reveals an increase in AP-1 activity compared to untreated cells (Figure 5.9). However, the AP-1 activity in PD98058 treated cells demonstrates less induction when compared to single erlotinib treatment. Furthermore, co-stimulation of erlotinib and PD98058 of primary human keratinocytes results in an induction of AP-1 activity similar to single erlotinib treatment (Figure 5.9).

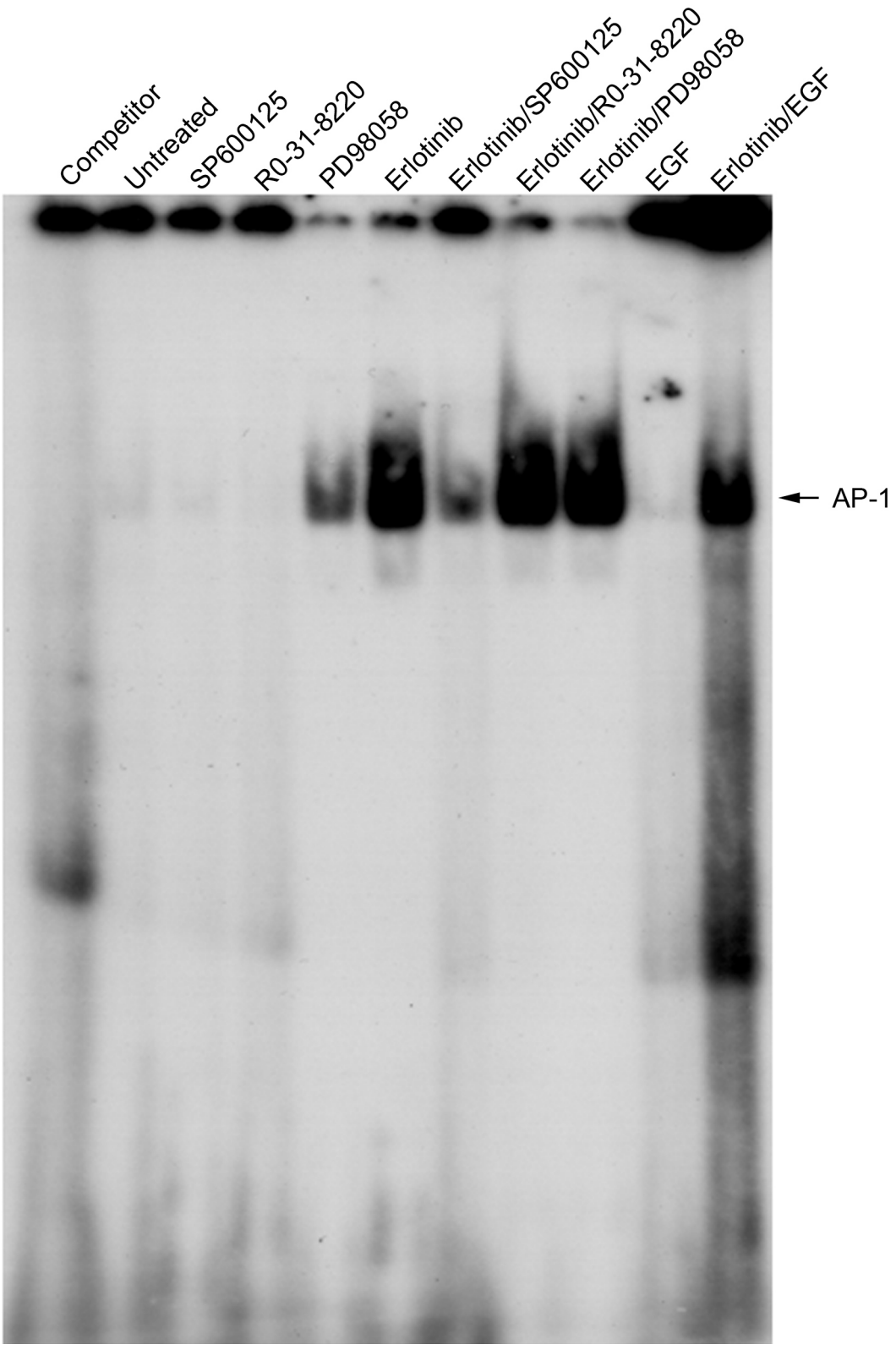

Figure 5.9 EMSA assay using radioactively labeled oligonucleotides containing the AP-1 consensus. AP-1 activity is increased in erlotinib treated primary human keratinocytes as compared to untreated cells. Inhibitory studies with SP600125 (JNK inhibitor) and PD98059 (Erk1/2 inhibitor) demonstrate the importance of JNK/AP-1 pathway. Shown are representative results of n=3 independent experiments.

5.10 Rational-based therapy

Analyses indicate that EGFR-I treatment results in enhanced inflammation and reduced host defense within the skin. Hence, it was investigated whether anti-inflammatory and/or antibiotic strategies may rescue EGFR-I induced alterations at the molecular level and may therefore result in the clinical improvement of cutaneous symptoms.

First, a glucocorticosteroid (mometason furoate)-containing cream (Ecural®, Essex Pharma GmbH, Munich, Germany) was topically applied to the lesional skin of EGFR-I treated patients twice daily to modulate the inflammatory aspect of EGFR-I associated adverse events. Assessment of the rash severity score (ERSS) of 21 patients prior to therapy initiation and after 3 weeks reveals that the mean ERSS significantly improves from 45.87 to 26.99 (P=0.00009, Student's t-test) (Figure 5.10.1 A).

Second, a combined approach was conducted targeting the inflammatory as well as the infectious facet of the rash. In this study, 23 patients were treated concomitantly with nadifloxacin cream (Nadixa®, Dr. R. Pfleger Chemische Fabrik GmbH, Bamberg, Germany), a potent topical fluoroquinolone antibiotic with a broad-spectrum activity against gram-positive and gram-negative bacteria and the topical glucocorticosteroid prednicarbate 0.25% cream (Dermatop®, Sanofi Aventis, Frankfurt, Germany). The mean ERSS improved significantly from 30.96 to 24.11 (P=0.030, Student's t-test) after 3 weeks of therapy (Figure 5.10.1 B).

Third, the retinoid isotretinoin (Aknenormin®, Almirall-Hermal, Barcelona, Spain) which represents a standard option for the systemic treatment of papulo-pustular skin diseases like acne or rosacea, was considered. *In vitro*, isotretinoin significantly impairs EGFR-I induced overexpression of the proinflammatory chemokines CXCL14 and CCL5 in cultured human primary keratinocytes.

To analyze the cellular and molecular mechanisms of isotretinoin in the management of EGFR-I rashes primary human keratinocytes were treated with erlotinib (1000 nM) in the presence or absence of isotretinoin (1000 nM). In fact, isotretinoin significantly (P=0.009, Student's t-test) impairs the induction of

CXCL14 by erlotinib (Figure 5.10.2). Notably, treatment with isotretinoin is also capable of impairing the erlotinib induced CCL5 expression (Figure 5.10.2).

To now assess the clinical efficacy of systemic isotretinoin in the management of the rash, 5 patients that presented with severe papulo-pustular eruptions (ERSS > 50) were orally treated with isotretinoin (30 mg/day) and their rash severity was assessed. The mean ERSS significantly improved from 59.02 to 43.48 (P=0.015, Student's t-test) after 3 weeks of isotretinoin therapy supporting our *in vitro* findings (Fig. 5.9.1 B).

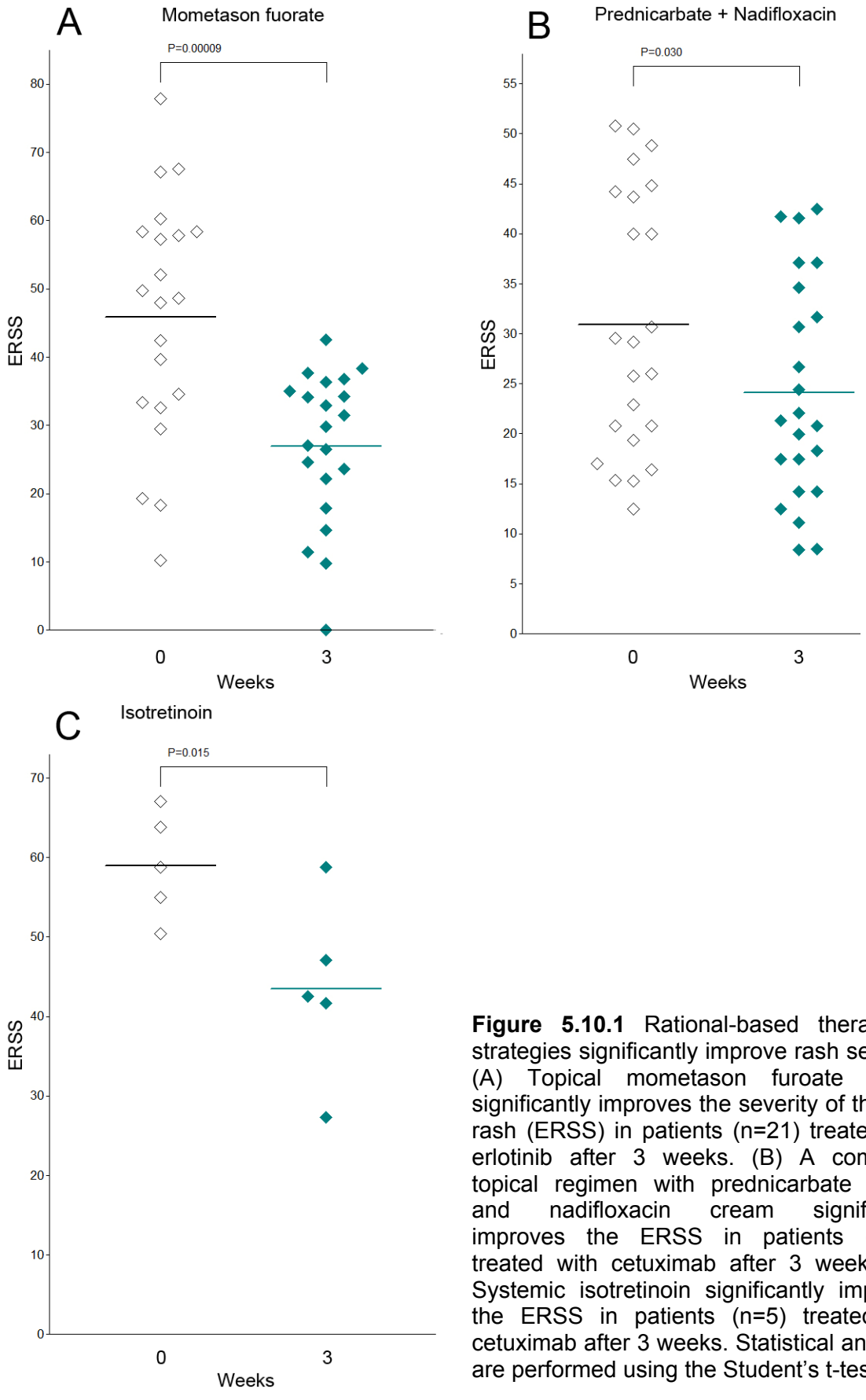

Figure 5.10.1 Rational-based therapeutic strategies significantly improve rash severity. (A) Topical mometason furoate cream significantly improves the severity of the skin rash (ERSS) in patients (n=21) treated with erlotinib after 3 weeks. (B) A combined topical regimen with prednicarbate cream and nadifloxacin cream significantly improves the ERSS in patients (n=23) treated with cetuximab after 3 weeks. (C) Systemic isotretinoin significantly improves the ERSS in patients (n=5) treated with cetuximab after 3 weeks. Statistical analyses are performed using the Student's t-test.

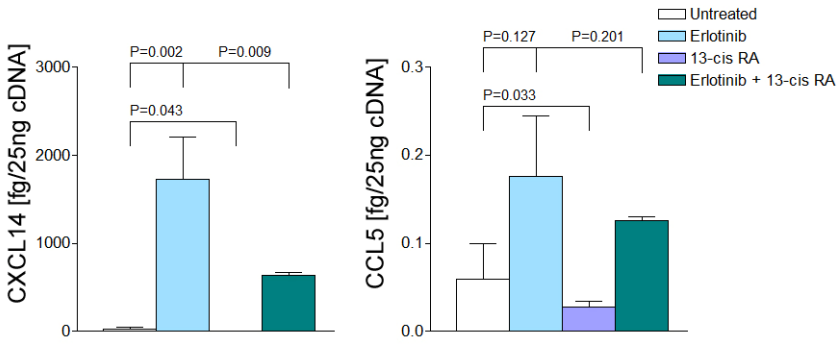

Figure 5.10.2 Effect of isotretinoin (13-cis RA) on EGFR-I induced chemokine induction. CXCL14 and CCL5 are induced in human keratinocytes treated with the EGFR-I erlotinib (1000 nM). When the retinoid isotretinoin (13-cis RA) (1000 nM) is co-administered with erlotinib treatment chemokine induction is reduced. Values are expressed as femtograms of target gene per 25 ng cDNA and represent the mean ± SD of three independent experiments (Student's t-test).

5.11 EGFR-I induced mast cell accumulation

Beside the characteristic papulo-pustular rashes, common side effects of EGFR-I treatment also include itching (pruritic) skin. Histochemical analyses of skin samples of lesional skin treated with the EGFR-I erlotinib reveal a marked clustering of mast cells in the periadnexial regions (Figure 5.11 A, B). Immunohistochemical analyses demonstrate specific mast cell tryptase staining (Figure 5.11 C, D). Additional quantification analyses by Image J reveal a significant (P=0.011, Student's t-test) accumulation of mast cells in EGFR-I treated patients (n=5) as compared to healthy controls (n=5) (Figure 5.11 D). Finally, expression analyses of stem cell factor (SCF) mRNA in primary human keratinocytes treated with erlotinib *in vitro* demonstrate a significant and dose-dependent induction of SCF (Figure 5.11 E) (Gerber, Buhren et al. 2009).

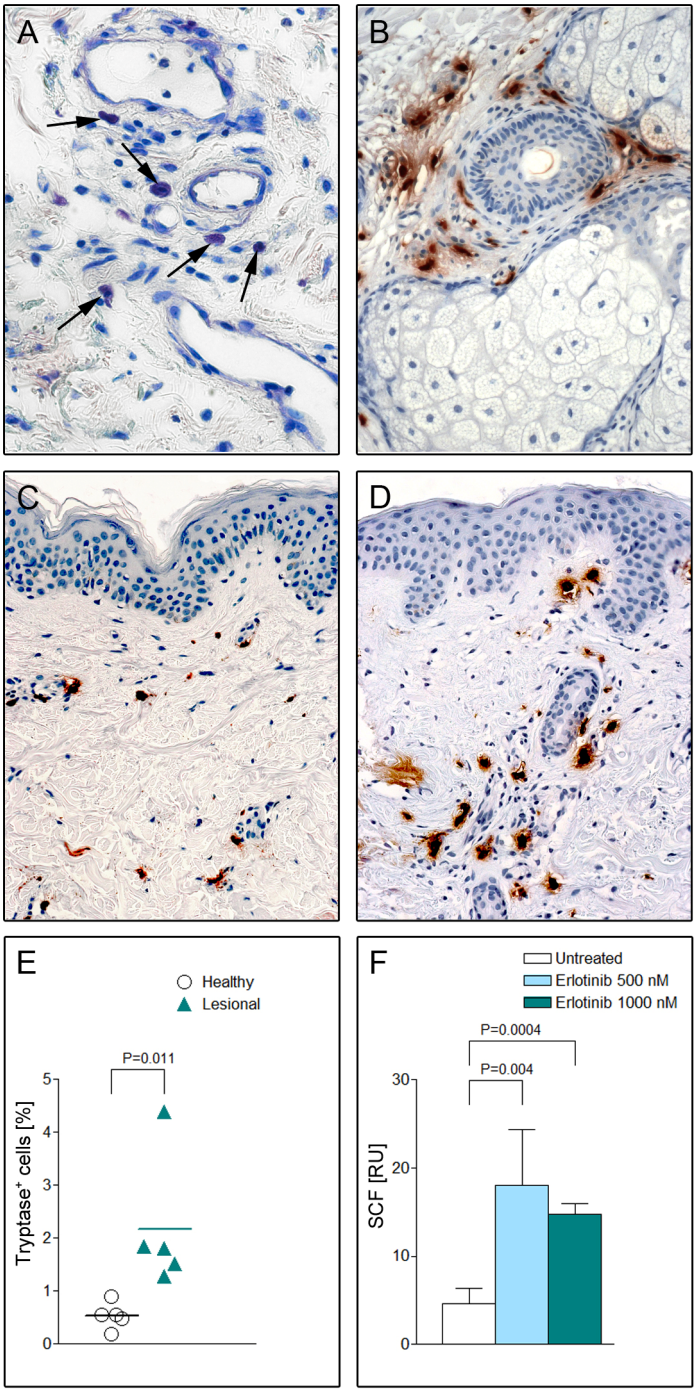

Figure 5.11 Mast cells accumulate in the periadnexial region of lesional skin in patients treated with erlotinib. (A, B) Giemsa staining. Mast cells are indicated by arrows. (C, D) Immunohistochemical analyses of anti mast cell tryptase in the skin of (C) healthy controls vs. (D) lesional skin of erlotinib treated patients. (E) Computer-assisted quantification demonstrates a significant induction of mast cell tryptase immunoreactivity in samples of erlotinib-induced rash (n=5) as compared to healthy skin (n=5). Values are indicated as percentages of tryptase positive cells per area. Statistical analyses are performed using the Student's t-test. (F) Erlotinib (500 nM, 1000 nM) induces a significant and dose-dependent overexpression of stem cell factor (SCF) in primary human keratinocytes. Values are expressed as relative units [RU] and represent the mean ± SD of three independent experiments (Student's t-test).

5.12 EGFR-I interferes with cutaneous wound healing

In order to investigate the role of EGFR-I in cutaneous wound healing, scratch assay analyses were performed. Notably, migratory responses toward scratches in those cells treated with the EGFR-I erlotinib are reduced. However, in untreated conditions the scratch in the monolayer of primary human

keratinocytes is completely closed by migrating cells following an incubation of 12 h, (Figure 5.12 B). Quantitative analyses of wound healing assays reveal that erlotinib could significantly impair wound healing in primary human keratinocytes (Figure 5.12 A). Additionally treatment with 1000 nM erlotinib impair scratch closure in cutaneous wound healing scratch assays using normal dermal human fibroblasts (NHDF) (Figure 5.12 C, D).

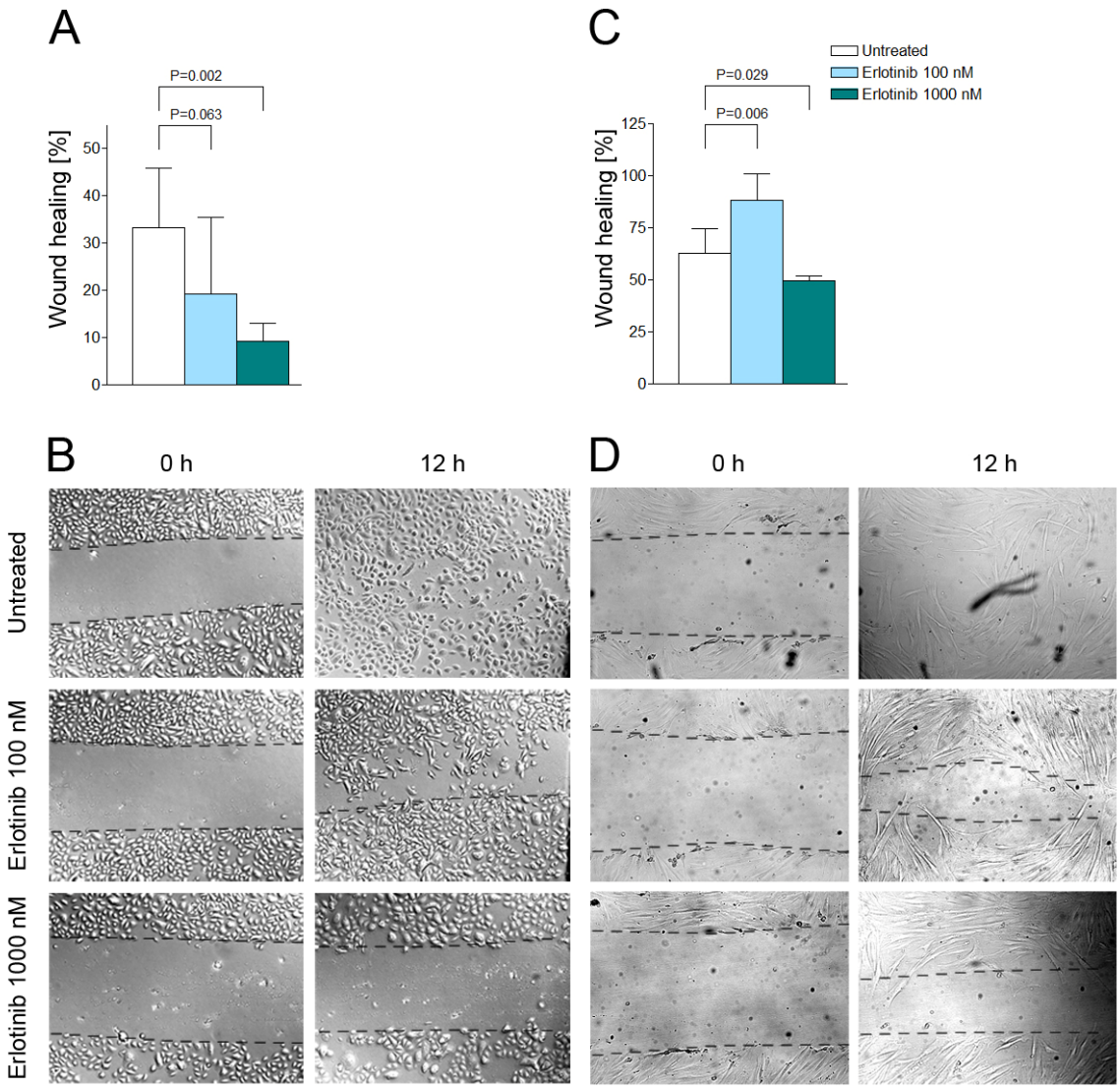

Figure 5.12 Cutaneous wound healing is decreased in cells treated with EGFR-I. Erlotinib significantly reduces wound healing in (A) primary human keratinocytes and (C) normal human dermal fibroblasts (NHDF). Wound scratches in erlotinib treated (B) primary human keratinocytes and (D) NHDF (1000 nM) fail to completely close after an incubation time of 12 h. The widths of the wound scratches at different time points are measured and expressed as a percentage of the initial distance at t=0. Results represent the mean ± SD of five independent experiments (Student's t-test).

6 Discussion

Dysregulation of the EGFR signaling pathway either via elevated expression level or through mutation is critically involved in the molecular pathogenesis of cancer (Jorissen *et al.* 2003, Yarden & Sliwkowski 2001). In fact, amplification or increased transcription of the EGFR gene, leading to an overexpression, has been detected in a broad variety of different solid human cancers (Salomon *et al.* 1995). Therefore, antagonists targeting the EGFR have emerged as a robust anti-neoplastic therapy (Hynes & Lane 2005). Although the safety profile of EGFR targeting cancer drugs is usually better than that of conventional chemotherapies (HeidaryNaik & Burgin 2008), it is now well recognized that they are not devoid of adverse effects. Cutaneous side-effects are the most frequent toxicities (Hu *et al.* 2007), which may significantly impair the quality of life and therefore bear a severe threat to patient compliance, as EGFR-I treatment can be interrupted or discontinued. Adverse effects include extensive papulo-pustular eruptions that are characterized by follicular-based erythematous papules and pustules (rash), dry skin (xerosis cutis), pruritus, paronychia, hair changes, and telangiectasia (Agero *et al.* 2006). Despite their clinical relevance the underlying cellular and molecular mechanisms of these EGFR-I associated adverse events have remained largely elusive and today no rational-based management strategies do exist.

Histological data indicate that the rash may be caused by EGFR inhibition in the skin, although this had yet to be confirmed. In order to validate whether the EGFR signaling pathway is impaired in skin lesions of erlotinib treated patients, immunohistochemical analyses of the activated form of EGFR (phospho-EGFR) and of the EGFR downstream target, Erk (phospho-Erk) were performed. Results demonstrate a reduced staining against phospho-EGFR and phospho-Erk in skin samples obtained from patients under therapy with erlotinib as compared to skin samples obtained from healthy volunteers. This indicates the strong EGFR-antagonizing activity of erlotinib within the skin and implies that cutaneous adverse effects are a result of direct drug activity rather than indirect metabolic effects.

In the skin the EGFR is primarily expressed by undifferentiated, proliferating keratinocytes of the basal and suprabasal layers of the epidermis as well as the outer root sheath of hair follicles (Green *et al.* 1983, Green & Couchman 1984,

Hansen *et al.* 1997). Interestingly, it is demonstrated that the mixed inflammatory infiltrate of the EGFR-I induced rash is confined to the periadnexial region and therefore correlates to the localization of EGFR expression. Immunohistochemical analyses of early papulous stages of the EGFR-I rash show that this infiltrate was dominated by $CD68^+$ macrophages, intraepidermal $CD1a^+$ Langerhans cells as well as distinct subsets of T lymphocytes. As opposed to previous studies that describe the infiltrate of EGFR-I induced pustules to be dominated by neutrophilic granulocytes, it is here found that in the initial papulous stages, the infiltrate is dominated by effector T cells ($CD4^+ > CD8^+$). Accordingly, it is likely that EGFR-I associated pustules are the result of a T cell-driven neutrophilic inflammation. The inflammatory cascade observed during EGFR-I induced skin eruptions is reminiscent of findings in drug-induced acute generalized eruptive pustulosis (AGEP) where drug-specific T cells initiate the inflammatory response that finally develops into a pustulosis (Britschgi *et al.* 2001).

Next the function of chemokines in the context of cellular and molecular mechanisms that recruit inflammatory cells to lesional skin of EGFR-I treated patients was analyzed. Chemokines are a superfamily of small cytokine-like proteins that critically regulate the trafficking of distinct leukocytes subsets including lymphocytes, DCs, monocytes, and neutrophils. Strikingly, it is demonstrated that the systemic treatment with EGFR-I impairs EGFR signaling and results in the upregulation of a distinct set of skin-associated chemokines, such as CCL27, CXCL14 and CCL5. In the skin, the expression profile of these chemokines does not only match the localization of the inflammatory infiltrate but also the predominant expression of the EGFR in the keratinocytes of the basal layers of the epidermis and the outer root sheath of the hair follicles.

Furthermore, it is demonstrated that the EGFR-I erlotinib significantly induce the expression of proinflammatory and skin-associated chemokines such as CCL2, CCL5, CXCL9, CXCL10. In fact, the massive skin infiltration by T cells and macrophages is consistent with this specific chemokine expression profile. Epidermal CCL2 is involved in the early response to injury or irritants, and in T cell-mediated skin disorders like psoriasis or atopic dermatitis (Giustizieri et al. 2001, KimLee & Kang 2003). It also is involved in controlling the recruitment of monocytes/macrophages, dendritic cells, and T cells (Carr et al. 1994,

NakamuraWilliams & Kupper 1995). Therefore, T cell infiltration observed in EGFR-I rashes is likely attributable to the induction of CCL2. This is in line with recent findings were blocking anti-CCL2 antibodies inhibit leukocyte migration induced by inhibition of the EGFR (Hoffmann et al. 2009). However, the active immigration of T cells, monocytes, as well as neutrophils is also supported by the increased expression of CCL5 (Goebeler et al. 2001). In addition, type 1 cells, a subgroup of T helper cells, appear to be markedly recruited to the skin due to the release of the CXCR3 ligands, CXCL9 and CXCL10 by keratinocytes (Flier et al. 1999). Accordingly, in mouse models of irritant contact dermatitis and allergic contact dermatitis, EGFR inhibition leads to the aggravation of the inflammatory response of the skin, with upregulated chemokine expression and massive skin infiltration by T cells and macrophages similar to infiltrates of EGFR-I skin lesions (Pastore & Mascia 2008).

Interestingly, qPCR analyses demonstrate a significant erlotinib induced expression of CCL27. CCL27 is selectively produced in skin by epidermal keratinocytes and is one of two known ligands for CCR10, a chemokine receptor expressed by a subset of skin-homing memory T cells (Homey et al. 2002, Homey *et al.* 2000, Morales *et al.* 1999). In fact, it is shown that blocking EGFR signaling strongly induces CCL27 expression not only *in vitro* but also *in vivo*. Most interestingly, serum samples of erlotinib-treated patients demonstrate significantly increased CCL27 protein levels as compared to sera obtained from healthy individuals. CCL27 levels even exceed serum contents in patients suffering from chronic T cell mediated inflammatory diseases such as atopic dermatitis (AD) and psoriasis vulgaris (PsV) (Kakinuma *et al.* 2003). The importance of this finding is stressed by the fact that CCL27 is shown to positively correlate with disease severity (Nakazato *et al.* 2008) and is used as a disease specific marker in AD patients (Hijnen *et al.* 2004). Today the most specific marker for therapy / tumor response in EGFR-I patients is the time-consuming assessment of rash severity, which is directly correlated to the experience of the referring clinician (Herbst et al. 2005, Wollenberg et al. 2008). Alarmingly, more easy accessible, “objective” markers have not yet been identified. The results of this study now for the first time indicate that CCL27 serum content might qualify as such a marker. Interestingly, CCL27 might not only indirectly correlate to therapy response via a potential link to rash severity

but might also have a direct effect on tumor progression. This hypothesis is supported by recent findings which demonstrate a link between CCL27 expression and tumor immune escape (Pivarcsi *et al.* 2007). Herein, Pivarcsi et al. demonstrate that the activation of EGFR-Ras signaling pathways in keratinocyte-derived malignancies resulted in the progressive loss of CCL27 production, representing a mechanism of tumor cells to evade from the immune system (Pivarcsi *et al.* 2007). Yet, further studies need to be conducted to analyze the correlation of CCL27 serum content and rash severity on the one hand and the direct effect of CCL27 on tumor progression on the other hand.

Strikingly, the strongest chemokine induction following EGFR inhibition is observed for CXCL14. Although CXCL14 has been shown to chemoattract both activated monocytes (Sleeman *et al.* 2000) and immature dendritic cells (Shellenberger *et al.* 2004), the biological function of this chemokine remains still largely elusive and the receptor for CXCL14 has yet to be identified. Therefore, the link of CXCL14 and EGFR signaling was systematically analyzed. A DNA database analysis identified an AP-1 binding site within the putative promoter region of CXCL14. The AP-1 complex is composed of both homo- and heterodimers of the Jun and Fos families of transcription factors (Angel & Karin 1991). When stimulated, AP-1 binds to specific transactivation promoter regions or TREs (12-O-tetradecanoylphorbol 13-acetate responsive elements) on DNA to induce transcription of genes involved in cell proliferation, metastasis, and metabolism (Angel *et al.* 1987). Amongst others, the mitogen-activated protein kinase (MAPK) signaling pathways are critically involved in the regulation of AP-1 function (Karin 1995). In the epidermis AP-1 is known to be involved in regulating differentiation, carcinogenesis, UV response, photo-aging, and wound repair processes (Zenz & Wagner 2006). Recently, the deregulation of Jun/AP-1 complex has been linked to TNF-α-dependent skin inflammation in mice (Guinea-Viniegra *et al.* 2009). *In vitro* analyses of the DNA-binding activity of AP-1 complex demonstrate increased AP-1 activity in EGFR-I treated primary human keratinocytes. These findings strongly suggest a role of EGFR-I in regulating CXCL14 expression through AP-1. Moreover, data obtained from inhibitory experiments using the pharmacological inhibitors of extracellular signal-regulated kinase (Erk1/2) mitogen-activated protein kinase (MAPK), and

c-Jun-NH2-kinase (JNK) demonstrate the importance of the JNK/AP-1 pathway in the modulation of erlotinib-induced CXCL14 expression.

Next the biological relevance of CCL27 in the context of all chemotactic factors mediating the recruitment of T-cell subsets to EGFR-I induced inflammatory skin lesions was analyzed. Leukocyte Transwell chemotaxis assays clearly demonstrate a strong chemotactic effect for conditioned media obtained from primary human keratinocytes treated with erlotinib. Notably, neutralizing anti-CCL27 antibodies are capable of significantly impairing this migratory response in T cells, including $CD4^+$ and $CD8^+$ cell subsets. These findings are in line with recent observations that the neutralization of CCL27 impairs the recruitment of lymphocytes to the sites of 2,4-dinitro-1-fluorobenzene (DNFB)-induced contact dermatitis and ovalbumin-induced AD in mice (Homey et al. 2002). In summary, these results strongly suggest an important role of EGFR-I induced CCL27 production during the recruitment of effector T cells to sites of EGFR-I induced skin inflammation.

Yet, EGFR-I do not only induce but also suppress chemokine expression. In fact, our comprehensive analysis of the majority of the human chemokines revealed that EGFR-I negatively regulate the expression of tumor associated chemokines such as CXCL8 and CCL20. This is in line with recent observations of Mascia et al. that report that an enhanced CXCL8 expression is characteristically associated with EGFR activation (Mascia *et al.* 2003). CXCL8 has been shown to promote the growth and invasiveness behavior of malignant tumors. In addition, it has been reported that there is a direct correlation between high levels of CXCL8 and tumor angiogenesis, progression and metastasis of human cancer cells in murine nude xenografts models (Koch *et al.* 1992, Schadendorf *et al.* 1993, Xie 2001, Gerber *et al.* 2009). Similarly to CXCL8, CCL20 plays an important role in tumor chemokine network. CCL20 is thought to promote cancer progression either by acting directly as a growth factor on cancer cells or by establishing a microenvironment that represses anticancer responses (Raman *et al.* 2007). Despite the attraction of immature dendritic cells to the site of tumor, CCL20 overexpression is shown to enhance tumor growth and invasiveness (SchutyserStruyf & Van Damme 2003). Recently, CCL20 serum levels is found to be positively correlated with well

established tumor markers of nasopharyngeal carcinoma (NPC), implying that CCL20 might qualify as a novel serum marker for NPC detection and prediction of treatment outcome (Chang *et al.* 2008). Taken together, the present study provides novel insights into the anti-neoplastic effects of EGFR-I such as the suppression of tumor associated chemokines.

Additional complications associated with the use of EGFR-I include pruritus or pain. In a clinical study conducted by Boone and coworkers, patients frequently complain of physical symptoms associated with the rash such as itching and pain (Boone *et al.* 2007). In line with these clinical findings a marked periadnexial clustering of mast cells in lesional skin of EGFR-I treated patients was demonstrated (Gerber, Buhren et al. 2009). In inflamed skin, pruritus is often caused by the release of histamine from dermal mast cells (Ikoma *et al.* 2006). Quantification analyses reveal a 4-fold increase of mast cell density in EGFR-I treated patients as compared to healthy controls. Stem cell factor (SCF) is considered a major pivotal growth factor that facilitates the proliferation, sustains the survival, differentiation and maturation, and stimulates directional motility of mast cells (Okayama & Kawakami 2006). Strikingly, erlotinib significantly and dose-dependently induces SCF mRNA in primary human keratinocytes treated with erlotinib *in vitro.* In summary, this strongly suggests that pruritus in patients with EGFR-I is caused by mast cell accumulation due to EGFR-I mediated induction of SCF. Hence a feasible treatment option could be the application of topical calcineurin inhibitors such as pimecrolimus or tacrolimus, both of which have been considered highly specific and effective antagonists of mast cell mediator release (Ikoma et al. 2006). However, a need for additional studies to evaluate the value of calcineurin inhibitors in the management of the EGFR-I induced rash and in particular associated pruritus remains. Finally, the complex function of mast cells in the EGFR-I induced rash needs to be further elucidated.

Besides the above mentioned inflammatory reactions, EGFR-I patients exposed an increased frequency of cutaneous infections or colonizations, in particular with *S. aureus* (Table 4.1). Antimicrobial peptides (AMPs) such as human beta-defensins (HBDs) and cathelicidins expressed by keratinocytes are a critical component of the innate immune system to provide mammalian skin with

resistance to bacterial infections, viral pathogens, and fungi (Nizet et al. 2001). To gain insights into the high prevalence of cutaneous *S.aureus* infections in EGFR-I patients, a comprehensive expression analysis of AMPs in primary human keratinocytes in the presence of absence of EGFR-I was established. Analyses demonstrate that blocking the EGFR results in the suppression of RNase7, HBD3, and LL37 production which have been shown to be highly active against strains of *S. aureus* even at low micromolar concentrations (Harder et al. 2001, Harder & Schroder 2002). The functional relevance of these expression analyses is supported by recent observations of our lab that demonstrated that conditioned media of keratinocytes cultured in the presence of erlotinib exposed a significantly impaired cytotoxic activity against *S. aureus* as compared to medium treated controls (Data not shown.) This is in line with the observation that the increased susceptibility towards cutaneous infections with *S. aureus* is attributed to a decreased expression of AMPs (Ong *et al.* 2002). Moreover, a recent report indicates a defective upregulation of LL37 in atopic dermatitis upon wounding which might explain increased susceptibility towards cutaneous infection in particular by *S. aureus* (Wollenberg & Klein 2007). In summary, the frequent presence of *S. aureus* on the skin of patients treated with EGFR-I might reflect the absence of HBD3 and RNase7, the major keratinocyte-derived *S. aureus* killing AMPs of the human skin, on the skin of patients treated with EGFR-I (Harder et al. 2001, Harder & Schroder 2002, Schroder 2005).

Findings made in the skin may serve as model for extra-cutaneous adverse effects of EGFR. The abrogation of EGFR signaling in the gastrointestinal epithelium, for example, may result in inflammatory reactions and a deficient microbial host defense to cause the frequent EGFR-I associated diarrhea (Hartmann *et al.* 2009). Interestingly, a similar concept has been established for the pathogenesis of Crohn´s disease. Recent studies favor the hypothesis that Crohn´s disease is caused by a dysregulation of T cell mediated mucosal immunity and a reduced expression of intestinal AMPs (Wehkamp *et al.* 2005) . The mucosa in patients with Crohn´s disease is dominated by an infiltrate of $CD4^+$ T cells and a decreased expression of AMPs, including HBD3 and LL37, outlining a striking similarity to our findings in the skin. Moreover, the importance of AMPs such as LL37 for the control of systemic infections is

highlighted by additional recent studies. In a mouse pulmonary infections model the local overexpression of LL37 is associated to increased bacterial loads, whereas a systemic overexpression of LL37 decreased the mortality after bacterial challenges (Bals et al. 1999). Hence, it would be interesting to assess the potential role of infectious agents also in the pathogenesis of the frequent EGFR-I associated pneumonitis (Ciardiello & Tortora 2002). Based upon the findings in the skin an anti-inflammatory as well as antiseptic/antibiotic strategy to interfere with papulo-pustular EGFR-I induced cutaneous adverse events can be proposed. Accordingly, patients were subjected to either potent topical anti-inflammatory (mometason furoate cream) or combined topical less-potent anti-inflammatory (prednicarbate cream) and anti-infectious measures (nadifloxacin cream). Patients with higher clinical rash severity (ERSS > 50) received an additional systemic isotretinoin therapy, targeting the chemokine mediated recruitment of macrophages and lymphocytes the skin. Indeed, isotretinoin does not only impair the EGFR-I mediated induction of CXCL14 but also CCL5, implying the important role of this retinoid for the modulation of chemokine mediated lymphocyte trafficking in the skin.

Findings of this thesis suggest the following model for the pathogenesis of EGFR-I induced cutaneous adverse effects (Figure 6):

Under homeostatic conditions the EGFR serves as a central regulator of cutaneous inflammation and antimicrobial defence. Conversely, the pharmacologic inhibition of EGFR signaling enhances the production and release of a set of proinflammatory chemokines such as CCL27, CXCL14, and CCL5. These chemokines play an important role in the tissue-specific trafficking and recruitment of leukocyte subsets to the site of tissue inflammation. Recruited cell subsets include effector T cells ($CD4^+ > CD8^+$), dendritic cells and macrophages. Subsequently, activated monocytes, dendritic cells, and T cells release additional cytokines that activate resident inflammatory cells and lead to the development of erythematous papules. The recruitment of abundant neutrophilic granulocytes, finally, then results in the formation of the characteristic follicular pastules. Conversely, EGFR-I suppress the production of AMPs, including RNase7, HBD3, and LL37 which results in an impaired host defense and a subsequent increase of cutaneous and/or systhemic infections. Finally, cutaneous infections may serve as additional inflammatory stimuli to

promote/sustain EGFR-I driven inflammatory processes resulting in a self sustained circulus vitiosus.

Taken together, in this thesis a novel concept for the pathogenesis of inflammatory and infectious complications in patients treated with EGFR antagonists, as well as for the cellular and molecular mechanism of drugs applied in the management of these complications is presented. Findings may grant novel targets for the design of mechanism-based management strategies.

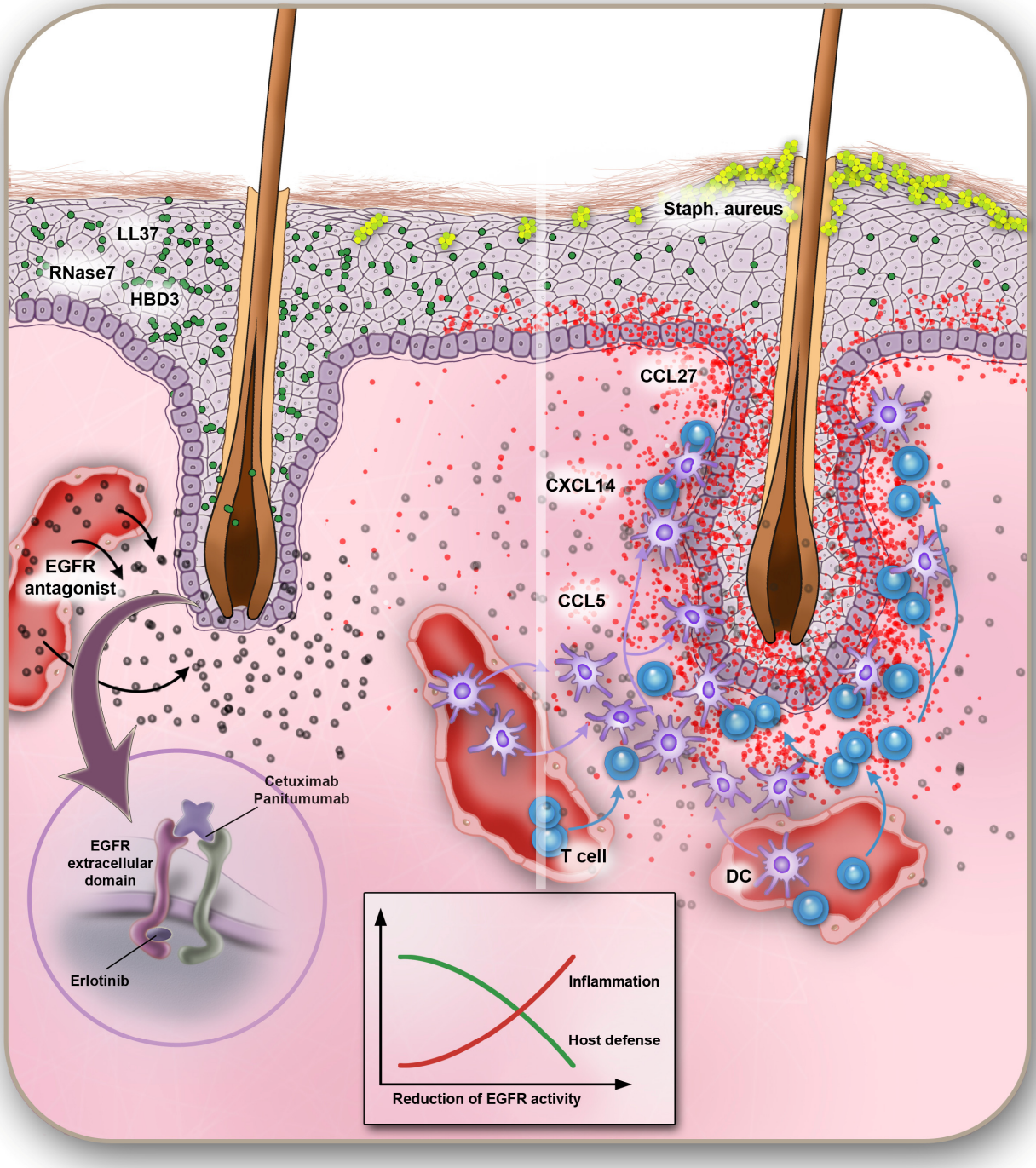

Figure 6 Proposed model for the pathogenesis of the cutaneous rash and associated infectious complications in patients treated with EGFR-I. EGFR-signaling critically controls cutaneous immune defense by modulating antimicrobial peptide (defensin) as well as chemokine production. *In vivo*, blockade of EGFR-signaling results in the down-regulation of epithelial antimicrobial peptides but up-regulation of skin-associated chemokine production, leading to cutaneous inflammation and decreased host defense with clinically relevant *S. aureus* infection.

7 References

FDA label information [online], <http://www.fda.gov/cder/foi/label/2004/021743lbl.pdf> (2004).

Agerberth, B., H. Gunne, J. Odeberg, P. Kogner, H. G. Boman & G. H. Gudmundsson (1995) FALL-39, a putative human peptide antibiotic, is cysteine-free and expressed in bone marrow and testis. *Proc Natl Acad Sci U S A,* **92,** 195.

Agero, A. L., S. W. Dusza, C. Benvenuto-Andrade, K. J. Busam, P. Myskowski & A. C. Halpern (2006) Dermatologic side effects associated with the epidermal growth factor receptor inhibitors. *J Am Acad Dermatol,* **55,** 657.

Angel, P., M. Imagawa, R. Chiu, B. Stein, R. J. Imbra, H. J. Rahmsdorf, C. Jonat, P. Herrlich & M. Karin (1987) Phorbol ester-inducible genes contain a common cis element recognized by a TPA-modulated trans-acting factor. *Cell,* **49,** 729.

Angel, P. & M. Karin (1991) The role of Jun, Fos and the AP-1 complex in cell-proliferation and transformation. *Biochim Biophys Acta,* **1072,** 129.

Arteaga, C. L. (2001) The epidermal growth factor receptor: from mutant oncogene in nonhuman cancers to therapeutic target in human neoplasia. *J Clin Oncol,* **19,** 32S.

Baggiolini, M. (2001) Chemokines in pathology and medicine. *J Intern Med,* **250,** 91.

Bals, R. (2000) Epithelial antimicrobial peptides in host defense against infection. *Respir Res,* **1,** 141.

Bianchi, S., D. Palli, M. Falchetti, C. Saieva, G. Masala, B. Mancini, R. Lupi, C. Noviello, J. Omerovic, M. Paglierani, V. Vezzosi, M. Alimandi, R. Mariani-Costantini & L. Ottini (2006) ErbB-receptors expression and survival in breast carcinoma: a 15-year follow-up study. *J Cell Physiol,* **206,** 702.

Boone, S. L., A. Rademaker, D. Liu, C. Pfeiffer, D. J. Mauro & M. E. Lacouture (2007) Impact and management of skin toxicity associated with anti-epidermal growth factor receptor therapy: survey results. *Oncology,* **72,** 152.

Bradford, M. M. (1976) A rapid and sensitive method for the quantitation of microgram quantities of protein utilizing the principle of protein-dye binding. *Anal Biochem,* **72,** 248.

Britschgi, M., U. C. Steiner, S. Schmid, J. P. Depta, G. Senti, A. Bircher, C. Burkhart, N. Yawalkar & W. J. Pichler (2001) T-cell involvement in drug-induced acute generalized exanthematous pustulosis. *J Clin Invest,* **107,** 1433.

Chang, K. P., S. P. Hao, J. H. Chang, C. C. Wu, N. M. Tsang, Y. S. Lee, C. L. Hsu, S. H. Ueng, S. C. Liu, Y. L. Liu, P. C. Wei, Y. Liang, Y. S. Chang & J. S. Yu (2008) Macrophage inflammatory protein-3alpha is a novel serum marker for nasopharyngeal carcinoma detection and prediction of treatment outcomes. *Clin Cancer Res,* **14,** 6979.

Charo, I. F. & R. M. Ransohoff (2006) The many roles of chemokines and chemokine receptors in inflammation. *N Engl J Med,* **354,** 610.

Ciardiello, F., R. Caputo, R. Bianco, V. Damiano, G. Fontanini, S. Cuccato, S. De Placido, A. R. Bianco & G. Tortora (2001) Inhibition of growth factor production and angiogenesis in human cancer cells by ZD1839 (Iressa), a selective epidermal growth factor receptor tyrosine kinase inhibitor. *Clin Cancer Res,* **7,** 1459.

Ciardiello, F. & G. Tortora (2002) Anti-epidermal growth factor receptor drugs in cancer therapy. *Expert Opin Investig Drugs,* **11,** 755.

Coussens, L., T. L. Yang-Feng, Y. C. Liao, E. Chen, A. Gray, J. McGrath, P. H. Seeburg, T. A. Libermann, J. Schlessinger, U. Francke & et al. (1985) Tyrosine kinase receptor with extensive homology to EGF receptor shares chromosomal location with neu oncogene. *Science,* **230,** 1132.

Dassonville, O., J. L. Formento, M. Francoual, A. Ramaioli, J. Santini, M. Schneider, F. Demard & G. Milano (1993) Expression of epidermal growth factor receptor and survival in upper aerodigestive tract cancer. *J Clin Oncol,* **11,** 1873.

Derynck, R., A. B. Roberts, M. E. Winkler, E. Y. Chen & D. V. Goeddel (1984) Human transforming growth factor-alpha: precursor structure and expression in E. coli. *Cell,* **38,** 287.

Dowell, J., J. D. Minna & P. Kirkpatrick (2005) Erlotinib hydrochloride. *Nat Rev Drug Discov,* **4,** 13.

Downward, J., Y. Yarden, E. Mayes, G. Scrace, N. Totty, P. Stockwell, A. Ullrich, J. Schlessinger & M. D. Waterfield (1984) Close similarity of epidermal growth factor receptor and v-erb-B oncogene protein sequences. *Nature,* **307,** 521.

Fearon, D. T. & R. M. Locksley (1996) The instructive role of innate immunity in the acquired immune response. *Science,* **272,** 50.

Frohm, M., B. Agerberth, G. Ahangari, M. Stahle-Backdahl, S. Liden, H. Wigzell & G. H. Gudmundsson (1997) The expression of the gene coding for the antibacterial peptide LL-37 is induced in human keratinocytes during inflammatory disorders. *J Biol Chem,* **272,** 15258.

Fulton, C., G. M. Anderson, M. Zasloff, R. Bull & A. G. Quinn (1997) Expression of natural peptide antibiotics in human skin. *Lancet,* **350,** 1750.

Gallo, R. L., M. Ono, T. Povsic, C. Page, E. Eriksson, M. Klagsbrun & M. Bernfield (1994) Syndecans, cell surface heparan sulfate proteoglycans, are induced by a proline-rich antimicrobial peptide from wounds. *Proc Natl Acad Sci U S A,* **91,** 11035.

Gerber, P. A., A. Hippe, B. A. Buhren, A. Muller & B. Homey (2009) Chemokines in tumor-associated angiogenesis. *Biol Chem*.

Gill, G. N., T. Kawamoto, C. Cochet, A. Le, J. D. Sato, H. Masui, C. McLeod & J. Mendelsohn (1984) Monoclonal anti-epidermal growth factor receptor antibodies which are inhibitors of epidermal growth factor binding and antagonists of epidermal growth factor binding and antagonists of epidermal growth factor-stimulated tyrosine protein kinase activity. *J Biol Chem,* **259,** 7755.

Goldstein, N. I., M. Prewett, K. Zuklys, P. Rockwell & J. Mendelsohn (1995) Biological efficacy of a chimeric antibody to the epidermal growth factor receptor in a human tumor xenograft model. *Clin Cancer Res,* **1,** 1311.

Gray, A., T. J. Dull & A. Ullrich (1983) Nucleotide sequence of epidermal growth factor cDNA predicts a 128,000-molecular weight protein precursor. *Nature,* **303,** 722.

Green, M. R., D. A. Basketter, J. R. Couchman & D. A. Rees (1983) Distribution and number of epidermal growth factor receptors in skin is related to epithelial cell growth. *Dev Biol,* **100,** 506.

Green, M. R. & J. R. Couchman (1984) Distribution of epidermal growth factor receptors in rat tissues during embryonic skin development, hair formation, and the adult hair growth cycle. *J Invest Dermatol,* **83,** 118.

Gropp, R., M. Frye, T. O. Wagner & J. Bargon (1999) Epithelial defensins impair adenoviral infection: implication for adenovirus-mediated gene therapy. *Hum Gene Ther,* **10,** 957.

Gschwind, A., O. M. Fischer & A. Ullrich (2004) The discovery of receptor tyrosine kinases: targets for cancer therapy. *Nat Rev Cancer,* **4,** 361.

Guinea-Viniegra, J., R. Zenz, H. Scheuch, D. Hnisz, M. Holcmann, L. Bakiri, H. B. Schonthaler, M. Sibilia & E. F. Wagner (2009) TNFalpha shedding and epidermal inflammation are controlled by Jun proteins. *Genes Dev,* **23,** 2663.

Hancock, R. E. & A. Rozek (2002) Role of membranes in the activities of antimicrobial cationic peptides. *FEMS Microbiol Lett,* **206,** 143.

Hansen, L. A., N. Alexander, M. E. Hogan, J. P. Sundberg, A. Dlugosz, D. W. Threadgill, T. Magnuson & S. H. Yuspa (1997) Genetically null mice reveal a central role for epidermal growth factor receptor in the differentiation of the hair follicle and normal hair development. *Am J Pathol,* **150,** 1959.

Harder, J., J. Bartels, E. Christophers & J. M. Schroder (1997) A peptide antibiotic from human skin. *Nature,* **387,** 861.

Harder, J., J. Bartels, E. Christophers & J. M. Schroder (2001) Isolation and characterization of human beta -defensin-3, a novel human inducible peptide antibiotic. *J Biol Chem,* **276,** 5707.

Harder, J. & J. M. Schroder (2002) RNase 7, a novel innate immune defense antimicrobial protein of healthy human skin. *J Biol Chem,* **277,** 46779.

Hartmann, J. T., M. Haap, H. G. Kopp & H. P. Lipp (2009) Tyrosine Kinase Inhibitors - A Review on Pharmacology, Metabolism and Side Effects. *Curr Drug Metab*.

Heidary, N., H. Naik & S. Burgin (2008) Chemotherapeutic agents and the skin: An update. *J Am Acad Dermatol,* **58,** 545.

Herbst, R. S., D. Prager, R. Hermann, L. Fehrenbacher, B. E. Johnson, A. Sandler, M. G. Kris, H. T. Tran, P. Klein, X. Li, D. Ramies, D. H. Johnson & V. A. Miller (2005) TRIBUTE: a phase III trial of erlotinib hydrochloride

(OSI-774) combined with carboplatin and paclitaxel chemotherapy in advanced non-small-cell lung cancer. *J Clin Oncol,* **23,** 5892.

Hidalgo, M., L. L. Siu, J. Nemunaitis, J. Rizzo, L. A. Hammond, C. Takimoto, S. G. Eckhardt, A. Tolcher, C. D. Britten, L. Denis, K. Ferrante, D. D. Von Hoff, S. Silberman & E. K. Rowinsky (2001) Phase I and pharmacologic study of OSI-774, an epidermal growth factor receptor tyrosine kinase inhibitor, in patients with advanced solid malignancies. *J Clin Oncol,* **19,** 3267.

Higashiyama, S., J. A. Abraham, J. Miller, J. C. Fiddes & M. Klagsbrun (1991) A heparin-binding growth factor secreted by macrophage-like cells that is related to EGF. *Science,* **251,** 936.

Hijnen, D., M. De Bruin-Weller, B. Oosting, C. Lebre, E. De Jong, C. Bruijnzeel-Koomen & E. Knol (2004) Serum thymus and activation-regulated chemokine (TARC) and cutaneous T cell- attracting chemokine (CTACK) levels in allergic diseases: TARC and CTACK are disease-specific markers for atopic dermatitis. *J Allergy Clin Immunol,* **113,** 334.

Homey, B., H. Alenius, A. Muller, H. Soto, E. P. Bowman, W. Yuan, L. McEvoy, A. I. Lauerma, T. Assmann, E. Bunemann, M. Lehto, H. Wolff, D. Yen, H. Marxhausen, W. To, J. Sedgwick, T. Ruzicka, P. Lehmann & A. Zlotnik (2002) CCL27-CCR10 interactions regulate T cell-mediated skin inflammation. *Nat Med,* **8,** 157.

Homey, B. & E. Bunemann (2004) Chemokines and inflammatory skin diseases. *Ernst Schering Res Found Workshop***,** 69.

Homey, B. & S. Meller (2008) Chemokines and other mediators as therapeutic targets in psoriasis vulgaris. *Clin Dermatol,* **26,** 539.

Homey, B., A. Muller & A. Zlotnik (2002) Chemokines: agents for the immunotherapy of cancer? *Nat Rev Immunol,* **2,** 175.

Homey, B., M. Steinhoff, T. Ruzicka & D. Y. Leung (2006) Cytokines and chemokines orchestrate atopic skin inflammation. *J Allergy Clin Immunol,* **118,** 178.

Homey, B., W. Wang, H. Soto, M. E. Buchanan, A. Wiesenborn, D. Catron, A. Muller, T. K. McClanahan, M. C. Dieu-Nosjean, R. Orozco, T. Ruzicka, P. Lehmann, E. Oldham & A. Zlotnik (2000) Cutting edge: the orphan chemokine receptor G protein-coupled receptor-2 (GPR-2, CCR10) binds

the skin-associated chemokine CCL27 (CTACK/ALP/ILC). *J Immunol,* **164,** 3465.

Hu, J. C., P. Sadeghi, L. C. Pinter-Brown, S. Yashar & M. W. Chiu (2007) Cutaneous side effects of epidermal growth factor receptor inhibitors: clinical presentation, pathogenesis, and management. *J Am Acad Dermatol,* **56,** 317.

Humphrey, P. A., A. J. Wong, B. Vogelstein, M. R. Zalutsky, G. N. Fuller, G. E. Archer, H. S. Friedman, M. M. Kwatra, S. H. Bigner & D. D. Bigner (1990) Anti-synthetic peptide antibody reacting at the fusion junction of deletion-mutant epidermal growth factor receptors in human glioblastoma. *Proc Natl Acad Sci U S A,* **87,** 4207.

Hynes, N. E. & H. A. Lane (2005) ERBB receptors and cancer: the complexity of targeted inhibitors. *Nat Rev Cancer,* **5,** 341.

Ikoma, A., M. Steinhoff, S. Stander, G. Yosipovitch & M. Schmelz (2006) The neurobiology of itch. *Nat Rev Neurosci,* **7,** 535.

Jacot, W., D. Bessis, E. Jorda, M. Ychou, M. Fabbro, J. L. Pujol & B. Guillot (2004) Acneiform eruption induced by epidermal growth factor receptor inhibitors in patients with solid tumours. *Br J Dermatol,* **151,** 238.

Jenssen, H., P. Hamill & R. E. Hancock (2006) Peptide antimicrobial agents. *Clin Microbiol Rev,* **19,** 491.

Jorissen, R. N., F. Walker, N. Pouliot, T. P. Garrett, C. W. Ward & A. W. Burgess (2003) Epidermal growth factor receptor: mechanisms of activation and signalling. *Exp Cell Res,* **284,** 31.

Kakinuma, T., H. Saeki, Y. Tsunemi, H. Fujita, N. Asano, H. Mitsui, Y. Tada, M. Wakugawa, T. Watanabe, H. Torii, M. Komine, A. Asahina, K. Nakamura & K. Tamaki (2003) Increased serum cutaneous T cell-attracting chemokine (CCL27) levels in patients with atopic dermatitis and psoriasis vulgaris. *J Allergy Clin Immunol,* **111,** 592.

Karin, M. (1995) The regulation of AP-1 activity by mitogen-activated protein kinases. *J Biol Chem,* **270,** 16483.

Koch, A. E., P. J. Polverini, S. L. Kunkel, L. A. Harlow, L. A. DiPietro, V. M. Elner, S. G. Elner & R. M. Strieter (1992) Interleukin-8 as a macrophage-derived mediator of angiogenesis. *Science,* **258,** 1798.

Kraus, M. H., W. Issing, T. Miki, N. C. Popescu & S. A. Aaronson (1989) Isolation and characterization of ERBB3, a third member of the ERBB/epidermal growth factor receptor family: evidence for overexpression in a subset of human mammary tumors. *Proc Natl Acad Sci U S A,* **86,** 9193.

Lehrer, R. I., A. K. Lichtenstein & T. Ganz (1993) Defensins: antimicrobial and cytotoxic peptides of mammalian cells. *Annu Rev Immunol,* **11,** 105.

Lowes, M. A., A. M. Bowcock & J. G. Krueger (2007) Pathogenesis and therapy of psoriasis. *Nature,* **445,** 866.

Mascia, F., V. Mariani, G. Girolomoni & S. Pastore (2003) Blockade of the EGF receptor induces a deranged chemokine expression in keratinocytes leading to enhanced skin inflammation. *Am J Pathol,* **163,** 303.

Mendelsohn, J. & J. Baselga (2006) Epidermal growth factor receptor targeting in cancer. *Semin Oncol,* **33,** 369.

Miettinen, P. J., J. E. Berger, J. Meneses, Y. Phung, R. A. Pedersen, Z. Werb & R. Derynck (1995) Epithelial immaturity and multiorgan failure in mice lacking epidermal growth factor receptor. *Nature,* **376,** 337.

Morales, J., B. Homey, A. P. Vicari, S. Hudak, E. Oldham, J. Hedrick, R. Orozco, N. G. Copeland, N. A. Jenkins, L. M. McEvoy & A. Zlotnik (1999) CTACK, a skin-associated chemokine that preferentially attracts skin-homing memory T cells. *Proc Natl Acad Sci U S A,* **96,** 14470.

Moyer, J. D., E. G. Barbacci, K. K. Iwata, L. Arnold, B. Boman, A. Cunningham, C. DiOrio, J. Doty, M. J. Morin, M. P. Moyer, M. Neveu, V. A. Pollack, L. R. Pustilnik, M. M. Reynolds, D. Sloan, A. Theleman & P. Miller (1997) Induction of apoptosis and cell cycle arrest by CP-358,774, an inhibitor of epidermal growth factor receptor tyrosine kinase. *Cancer Res,* **57,** 4838.

Murphy, P. M., M. Baggiolini, I. F. Charo, C. A. Hebert, R. Horuk, K. Matsushima, L. H. Miller, J. J. Oppenheim & C. A. Power (2000) International union of pharmacology. XXII. Nomenclature for chemokine receptors. *Pharmacol Rev,* **52,** 145.

Nakazato, J., M. Kishida, R. Kuroiwa, J. Fujiwara, M. Shimoda & N. Shinomiya (2008) Serum levels of Th2 chemokines, CCL17, CCL22, and CCL27, were the important markers of severity in infantile atopic dermatitis. *Pediatr Allergy Immunol,* **19,** 605.

Nishikawa, R., X. D. Ji, R. C. Harmon, C. S. Lazar, G. N. Gill, W. K. Cavenee & H. J. Huang (1994) A mutant epidermal growth factor receptor common in human glioma confers enhanced tumorigenicity. *Proc Natl Acad Sci U S A,* **91,** 7727.

Nizet, V., T. Ohtake, X. Lauth, J. Trowbridge, J. Rudisill, R. A. Dorschner, V. Pestonjamasp, J. Piraino, K. Huttner & R. L. Gallo (2001) Innate antimicrobial peptide protects the skin from invasive bacterial infection. *Nature,* **414,** 454.

Okayama, Y. & T. Kawakami (2006) Development, migration, and survival of mast cells. *Immunol Res,* **34,** 97.

Ong, P. Y., T. Ohtake, C. Brandt, I. Strickland, M. Boguniewicz, T. Ganz, R. L. Gallo & D. Y. Leung (2002) Endogenous antimicrobial peptides and skin infections in atopic dermatitis. *N Engl J Med,* **347,** 1151.

Pastore, S. & F. Mascia (2008) Novel acquisitions on the immunoprotective roles of the EGF receptor in the skin. *Expert Rev Dermatol,* **3,** 525.

Pastore, S., F. Mascia, F. Mariotti, C. Dattilo, V. Mariani & G. Girolomoni (2005) ERK1/2 regulates epidermal chemokine expression and skin inflammation. *J Immunol,* **174,** 5047.

Pedersen, M. W., M. Meltorn, L. Damstrup & H. S. Poulsen (2001) The type III epidermal growth factor receptor mutation. Biological significance and potential target for anti-cancer therapy. *Ann Oncol,* **12,** 745.

Perez-Soler, R., A. Chachoua, L. A. Hammond, E. K. Rowinsky, M. Huberman, D. Karp, J. Rigas, G. M. Clark, P. Santabarbara & P. Bonomi (2004) Determinants of tumor response and survival with erlotinib in patients with non--small-cell lung cancer. *J Clin Oncol,* **22,** 3238.

Pivarcsi, A., A. Muller, A. Hippe, J. Rieker, A. van Lierop, M. Steinhoff, S. Seeliger, R. Kubitza, U. Pippirs, S. Meller, P. A. Gerber, R. Liersch, E. Buenemann, E. Sonkoly, U. Wiesner, T. K. Hoffmann, L. Schneider, R. Piekorz, E. Enderlein, J. Reifenberger, U. P. Rohr, R. Haas, P. Boukamp, I. Haase, B. Nurnberg, T. Ruzicka, A. Zlotnik & B. Homey (2007) Tumor immune escape by the loss of homeostatic chemokine expression. *Proc Natl Acad Sci U S A,* **104,** 19055.

Plowman, G. D., J. M. Culouscou, G. S. Whitney, J. M. Green, G. W. Carlton, L. Foy, M. G. Neubauer & M. Shoyab (1993) Ligand-specific activation of

HER4/p180erbB4, a fourth member of the epidermal growth factor receptor family. *Proc Natl Acad Sci U S A,* **90,** 1746.

Plowman, G. D., G. S. Whitney, M. G. Neubauer, J. M. Green, V. L. McDonald, G. J. Todaro & M. Shoyab (1990) Molecular cloning and expression of an additional epidermal growth factor receptor-related gene. *Proc Natl Acad Sci U S A,* **87,** 4905.

Pollack, V. A., D. M. Savage, D. A. Baker, K. E. Tsaparikos, D. E. Sloan, J. D. Moyer, E. G. Barbacci, L. R. Pustilnik, T. A. Smolarek, J. A. Davis, M. P. Vaidya, L. D. Arnold, J. L. Doty, K. K. Iwata & M. J. Morin (1999) Inhibition of epidermal growth factor receptor-associated tyrosine phosphorylation in human carcinomas with CP-358,774: dynamics of receptor inhibition in situ and antitumor effects in athymic mice. *J Pharmacol Exp Ther,* **291,** 739.

Raman, D., P. J. Baugher, Y. M. Thu & A. Richmond (2007) Role of chemokines in tumor growth. *Cancer Lett,* **256,** 137.

Rossi, D. & A. Zlotnik (2000) The biology of chemokines and their receptors. *Annu Rev Immunol,* **18,** 217.

Salomon, D. S., R. Brandt, F. Ciardiello & N. Normanno (1995) Epidermal growth factor-related peptides and their receptors in human malignancies. *Crit Rev Oncol Hematol,* **19,** 183.

Sanderson, M. P., P. J. Dempsey & A. J. Dunbar (2006) Control of ErbB signaling through metalloprotease mediated ectodomain shedding of EGF-like factors. *Growth Factors,* **24,** 121.

Sasada, R., Y. Ono, Y. Taniyama, Y. Shing, J. Folkman & K. Igarashi (1993) Cloning and expression of cDNA encoding human betacellulin, a new member of the EGF family. *Biochem Biophys Res Commun,* **190,** 1173.

Sato, J. D., T. Kawamoto, A. D. Le, J. Mendelsohn, J. Polikoff & G. H. Sato (1983) Biological effects in vitro of monoclonal antibodies to human epidermal growth factor receptors. *Mol Biol Med,* **1,** 511.

Savage, C. R., Jr. & S. Cohen (1972) Epidermal growth factor and a new derivative. Rapid isolation procedures and biological and chemical characterization. *J Biol Chem,* **247,** 7609.

Schadendorf, D., A. Moller, B. Algermissen, M. Worm, M. Sticherling & B. M. Czarnetzki (1993) IL-8 produced by human malignant melanoma cells in vitro is an essential autocrine growth factor. *J Immunol,* **151,** 2667.

Schechter, A. L., D. F. Stern, L. Vaidyanathan, S. J. Decker, J. A. Drebin, M. I. Greene & R. A. Weinberg (1984) The neu oncogene: an erb-B-related gene encoding a 185,000-Mr tumour antigen. *Nature,* **312,** 513.

Schroder, J. M. (2005) The role of antimicrobial peptides and proteins in keratinocyte defense. *Exp Dermatol,* **14,** 783.

Schutyser, E., S. Struyf & J. Van Damme (2003) The CC chemokine CCL20 and its receptor CCR6. *Cytokine Growth Factor Rev,* **14,** 409.

Shellenberger, T. D., M. Wang, M. Gujrati, A. Jayakumar, R. M. Strieter, M. D. Burdick, C. G. Ioannides, C. L. Efferson, A. K. El-Naggar, D. Roberts, G. L. Clayman & M. J. Frederick (2004) BRAK/CXCL14 is a potent inhibitor of angiogenesis and a chemotactic factor for immature dendritic cells. *Cancer Res,* **64,** 8262.

Shoyab, M., G. D. Plowman, V. L. McDonald, J. G. Bradley & G. J. Todaro (1989) Structure and function of human amphiregulin: a member of the epidermal growth factor family. *Science,* **243,** 1074.

Sibilia, M. & E. F. Wagner (1995) Strain-dependent epithelial defects in mice lacking the EGF receptor. *Science,* **269,** 234.

Sleeman, M. A., J. K. Fraser, J. G. Murison, S. L. Kelly, R. L. Prestidge, D. J. Palmer, J. D. Watson & K. D. Kumble (2000) B cell- and monocyte-activating chemokine (BMAC), a novel non-ELR alpha-chemokine. *Int Immunol,* **12,** 677.

Sorensen, O. E., P. Follin, A. H. Johnsen, J. Calafat, G. S. Tjabringa, P. S. Hiemstra & N. Borregaard (2001) Human cathelicidin, hCAP-18, is processed to the antimicrobial peptide LL-37 by extracellular cleavage with proteinase 3. *Blood,* **97,** 3951.

Soulieres, D., N. N. Senzer, E. E. Vokes, M. Hidalgo, S. S. Agarwala & L. L. Siu (2004) Multicenter phase II study of erlotinib, an oral epidermal growth factor receptor tyrosine kinase inhibitor, in patients with recurrent or metastatic squamous cell cancer of the head and neck. *J Clin Oncol,* **22,** 77.

Stolzenberg, E. D., G. M. Anderson, M. R. Ackermann, R. H. Whitlock & M. Zasloff (1997) Epithelial antibiotic induced in states of disease. *Proc Natl Acad Sci U S A,* **94,** 8686.

Strachan, L., J. G. Murison, R. L. Prestidge, M. A. Sleeman, J. D. Watson & K. D. Kumble (2001) Cloning and biological activity of epigen, a novel member of the epidermal growth factor superfamily. *J Biol Chem,* **276,** 18265.

Sunada, H., B. E. Magun, J. Mendelsohn & C. L. MacLeod (1986) Monoclonal antibody against epidermal growth factor receptor is internalized without stimulating receptor phosphorylation. *Proc Natl Acad Sci U S A,* **83,** 3825.

Threadgill, D. W., A. A. Dlugosz, L. A. Hansen, T. Tennenbaum, U. Lichti, D. Yee, C. LaMantia, T. Mourton, K. Herrup, R. C. Harris & et al. (1995) Targeted disruption of mouse EGF receptor: effect of genetic background on mutant phenotype. *Science,* **269,** 230.

Toyoda, H., T. Komurasaki, Y. Ikeda, M. Yoshimoto & S. Morimoto (1995) Molecular cloning of mouse epiregulin, a novel epidermal growth factor-related protein, expressed in the early stage of development. *FEBS Lett,* **377,** 403.

Ullrich, A., L. Coussens, J. S. Hayflick, T. J. Dull, A. Gray, A. W. Tam, J. Lee, Y. Yarden, T. A. Libermann, J. Schlessinger & et al. (1984) Human epidermal growth factor receptor cDNA sequence and aberrant expression of the amplified gene in A431 epidermoid carcinoma cells. *Nature,* **309,** 418.

Wehkamp, J., M. Schmid, K. Fellermann & E. F. Stange (2005) Defensin deficiency, intestinal microbes, and the clinical phenotypes of Crohn's disease. *J Leukoc Biol,* **77,** 460.

Wells, A. (1999) EGF receptor. *Int J Biochem Cell Biol,* **31,** 637.

Wollenberg, A. & E. Klein (2007) Current aspects of innate and adaptive immunity in atopic dermatitis. *Clin Rev Allergy Immunol,* **33,** 35.

Wollenberg, A., N. Moosmann, E. Klein & K. Katzer (2008) A tool for scoring of acneiform skin eruptions induced by EGF receptor inhibition. *Exp Dermatol,* **17,** 790.

Xie, K. (2001) Interleukin-8 and human cancer biology. *Cytokine Growth Factor Rev,* **12,** 375.

Yarden, Y. & M. X. Sliwkowski (2001) Untangling the ErbB signalling network. *Nat Rev Mol Cell Biol,* **2,** 127.

Zenz, R. & E. F. Wagner (2006) Jun signalling in the epidermis: From developmental defects to psoriasis and skin tumors. *Int J Biochem Cell Biol,* **38,** 1043.

Zhao, C., I. Wang & R. I. Lehrer (1996) Widespread expression of beta-defensin hBD-1 in human secretory glands and epithelial cells. *FEBS Lett,* **396,** 319.

Zlotnik, A. & O. Yoshie (2000) Chemokines: a new classification system and their role in immunity. *Immunity,* **12,** 121.

Zlotnik, A., O. Yoshie & H. Nomiyama (2006) The chemokine and chemokine receptor superfamilies and their molecular evolution. *Genome Biol,* **7,** 243.

8 Abbreviations

%	per cent
°C	degree Celsius
µg	microgram
µl	microliter
AD	atopic dermatitis
ADAM	a disintegrin and metalloprotease
AEC	3-Amino-9-Ethyl-carbazol
AMP	antimicrobial peptide
AOD	assay on demand
AR	amphiregulin
ATP	Adenosine triphosphate
Bis-Tris	Bis(2-hydroxyethyl)amino-tris(hydroxymethyl)methan
BPE	bovine pituitary extract
BSA	bovine serum albumin
BTC	betacellulin
CAMP	cathelicidin antimicrobial protein
C-buffer	chemotaxis-buffer
CDK	cyclin dependent kinase
cDNA	complementary DNA
CFU	colony forming unit
CLA	cutaneous lymphocyte antigen
CRAMP	cathelin-related antimicrobial peptide
CTACK	cutaneous T cell-attracting chemokine
CTCAE	Common Terminology Criteria for Adverse Events
C_t-value	threshold cycle
Cy5	cyanine5
DCs	dendritic cells
ddH_2O	bidistilled water
DEPC	diethylpyrocarbonate
dH_2O	distilled water
DMSO	dimethyl sulfoxide

DNA	desoxyribonucleic acid
dNTP	deoxyribonucleotide triphosphate
DTT	dithiothreitol
ECL	enhanced luminol-based chemiluminescent
ECM	extracellular matrix
EDTA	ethylenediaminetetraacetic acid
EGF	epidermal growth factor
EGFR	epidermal growth factor receptor
EGFR-I	epidermal growth factor receptor-inhibitor
ELISA	enzyme-linked immunosorbent assay
EMSA	electrophoretic mobility shift assay
EPG	epigen
EPR	epiregulin
Erk	extracellular signal-regulated kinase
ERSS	EGFR-I-induced rash severity score
et al.	et alii (and others)
FACS	fluorescence activated cell sorting
fg	femtogram
FITC	fluorescein isothiocyanate
FSC	forward scatter
g	gram
GPCR	G protein-coupled receptor
h	hour(s)
H_2O	water
HBD	human beta defensin
HB-EGF	heparin-binding EGF-like growth factor
hCAP18	human cationic protein 18kDa
HCl	hydrogen chloride
HEPES	4-(2-hydroxyethyl)-1-piperazineethanesulfonic acid
HNC	head and neck
HNSCC	squamous cell carcinoma of the head and neck
HRP	horseradish peroxidase
IFN-γ	interferon-gamma

IgG	immunoglobulin G
IgM	immunoglobulin M
IL	interleukin
IP-10	interferon-inducible protein 10 kDa
IUPAC	International Union of Pure and Applied Chemistry
Jak/Stat	Janus kinases/signal transducers and activators of transcription
JNK	c-Jun N-terminal kinases
KCl	potassium chloride
kDa	kilo Dalton
KH_2PO_4	potassium dihydrogen phosphate
$KHCO_3$	potassium bicarbonate
M	molar
mAb	monoclonal antibody
MAP	mitogen-activated protein
MCP-1	monocyte chemotactic protein-1
mg	milligram
min	minute(s)
MIP-3α	macrophage inflammatory protein- alpha3
ml	milliliter
mM	millimolar
mm	millimeter
MMP	matrix metalloproteinases
MOPS	3-(N-morpholino)propanesulfonic acid
mRNA	messenger RNA
MW	molecular weight
ng	nanogram
Na_2-EDTA	disodium EDTA
Na_2HPO_4	sodium phosphate
NaCl	sodium chloride
NE cells	neutrophilic elastase
NH_4Cl	ammonium chloride
NHDF	normal human dermal fibroblast

nm	nanometer
nM	nanomolar
no.	number
NSCLC	non-small cell lung cancer
O.C.T.	optimal cutting temperature
o.n.	over night
OD	optical density
oligo(dt)	oligo(deoxythymidylic acid)
PBMC	peripheral blood mononuclear cell
PBS	phosphate buffer saline
PCR	polymerase chain reaction
PE	phycoerythrin
p-EGFR	phosphor-EGFR
p-Erk	phosphor-Erk
PFA	paraformaldehyde
pg	picogram
PsV	psoriasis vulgaris
PVDF	polyvinylidene fluoride
qPCR	quantitative real time PCR
RA	retinoid acid
RANTES	regulated upon activation, normal T cell expressed, and secreted
RNA	ribonucleic acid
rpm	rounds per minute
RPMI	Roswell Park Memorial Institute
rRNA	ribosomal RNA
RT	room temperature
RTK	receptor tyrosine kinase
RU	relative units
S. aureus	Staphylococcus aureus
SCF	stem cell factor
SD	standard deviation
SDS	sodium dodecyl sulfate

SDS-PAGE	SDS-polyacrylamide gel electrophoresis
SSC	side scatter
t	time
TBS	tris buffered saline
TBS-T	TBS- Tween® 20
TGF-α	transforming growth factor alpha
TKI	tyrosine kinase inhibitor
TNF-α	tumor necrosis factor-alpha
Tris-base	trishydroxymethylaminomethane-base
Tween® 20	polyoxyethylene (20) sorbitan monolaurate
U	units
V	voltage
w/v	weight per volume
yr	year
Δ	delta

Acknowledgements

I would like to express my sincere gratitude and thanks to my supervisor Prof. Dr. Bernhard Homey for giving me the opportunity to carry out this fascinating research. I appreciate the interesting discussions and expert scientific guidance.

My special thanks are also due to Prof. Dr. Dieter Willbold for co-advising this work.

I am very grateful to Dr. Peter Arne Gerber who guided me through all steps of this project with patience. He provided me with advices, valuable suggestions and continuous encouragement.

There are members of the lab but also good friends who contributed to this work in so many different ways. Thank you for always being there whenever I needed your help.

Last but not least, I would like to express my special appreciation to my parents for giving me love, constant support, and most important – always demonstrating confidence in me.

Declaration

I declare that this thesis was composed by myself and that I exclusively used the indicated literature and resources. The thoughts taken directly or indirectly from external sources are properly marked as such.